

Role of estrogen in wound healing
through regulation of epithelial-
mesenchymal transition in human
keratinocyte

Jung U Shin

Department of Medicine

The Graduate School, Yonsei University

Role of estrogen in wound healing
through regulation of epithelial-
mesenchymal transition in human
keratinocyte

Jung U Shin

Department of Medicine

The Graduate School, Yonsei University

Role of estrogen in wound healing
through regulation of epithelial-
mesenchymal transition in human
keratinocyte

Directed by Professor Kwang Hoon Lee

The Doctoral Dissertation
submitted to the Department of Medicine,
the Graduate School of Yonsei University
in partial fulfillment of the requirements for the degree
of Doctor of Philosophy

Jung U Shin

Dec 2013

This certifies that the Doctoral
Dissertation of Jung U Shin is approved.

Thesis Supervisor: Prof. Prof. Kwang Hoon Lee

Thesis Committee Member: Prof. Dong Kyun Rah

Thesis Committee Member: Prof. Jong Shin Yoo

Thesis Committee Member: Prof. Kunhong Kim

Thesis Committee Member: Prof. Ju Hee Lee

The Graduate School
Yonsei University

Dec 2013

ACKNOWLEDGEMENTS

I very much appreciate my thesis supervisor, professor Kwang Hoon Lee, for his supervision and encouragement to study this subject.

I appreciate professors Dong Kyun Rah, Jong Shin Yoo, Kunhong Kim, Ju Hee Lee who gave me experienced advice and warm support. I also thank professor Jinyoung Kim, professor Won Jai Lee, professor Sang Ho Oh, professor Do Young Kim, Hyeran Kim, Inhee Jung, Ji Yeon Noh, Yun Sun Lee, Dr.Jung Soo Lee and Dr.Hemin Lee for great support.

I am truly grateful to my family members, especially my parents, my husband, and my two sons, who have been my side with love during the years of my study. I give my love and admiration to them.

<TABLE OF CONTENTS>

ABSTRACT	1
I. INTRODUCTION	4
II. MATERIALS AND METHODS	6
1. Cell culture	6
2. Treatments	6
3. Immunofluorescence	7
4. Cell viability assay	8
5. Semi-quantitative and quantitative real-time polymerase chain reaction (PCR)	8
6. Immunoblot analysis	10
7. Scratch assay	11
8. Cell migration assay	11
9. Stable isotope labeling by amino acids in cell culture (SILAC)	12
10. Transfection of small interfering RNAs	17
11. Statistics	18
III. RESULTS	19
1. Expression of estrogen receptor α and β in HaCaT cells	19
2. Effect of E2 on the viability of HaCaT cells	21
3. Estrogen modulated EMT-related molecules in HaCaT cells	22
4. Effects of estrogen on EMT-related molecules through the ER	25
5. Estrogen stimulates migration of HaCaT cells	26
6. Slug knockdown impairs the migration of HaCaT cells	29
7. Slug knockdown modulates E-cadherin and vimentin	32
8. Proteome alterations following E2 treatment as revealed by SILAC	33
9. Estrogen increases HMGB1 expression via the estrogen receptor	42
10. Alteration in HMGB1 level following Slug siRNA transfection	45

11. Addition of recombinant HMGB1 accelerates HaCaT cell migration	46
12. HMGB1 is important in the migration of HaCaT cells	47
IV. DISCUSSION	49
V. CONCLUSION	54
REFERENCES	56
ABSTRACT (IN KOREAN)	68

LIST OF FIGURES

Figure 1. Schematic diagram of general experimental procedure of SILAC	13
Figure 2. Expression of estrogen receptors (ERs) in HaCaT cells and primary human keratinocytes (PHK)	20
Figure 3. Cell viability as determined using MTT assay	21
Figure 4. Up-regulated Slug, Twist, and vimentin and down-regulated E- cadherin in HaCaT cells after treatment with E2	23
Figure 5. Estrogen receptor (ER) mediates E2-induced E-cadherin, vimentin, Slug, and Twist expression in HaCaT cells	25
Figure 6. Estrogen promotes the migration of HaCaT cells	27
Figure 7. Knockdown of Slug inhibits the migration of HaCaT cells	30
Figure 8. Up-regulated vimentin and down-regulated E-cadherin after Slug siRNA transfection	32
Figure 9. SILAC protein identification	40
Figure 10. E2 induces HMGB1 expression	43
Figure 11. Down-regulation of HMGB1 after Slug siRNA transfection ...	45
Figure 12. Increased migration of HaCaT cells after treatment with HMGB1	46
Figure 13. Knockdown of HMGB1 inhibits the migration of HaCaT cells	48

LIST OF TABLES

Table 1. Thirty-two down-regulated ($p < 0.05$) proteins after 17β -estradiol treatment in HaCaT cells	34
Table 2. Sixty up-regulated ($p < 0.05$) proteins after 17β -estradiol treatment in HaCaT cells	36
Table 3. Six up-regulated (protein ratio > 1.2) high mobility group proteins after 17β -estradiol treatment in HaCaT cells	39

ABSTRACT

Role of estrogen in wound healing through regulation of epithelial-mesenchymal transition in human keratinocytes

Jung U Shin

*Department of Medicine
The Graduate School, Yonsei University*

(Directed by Professor Kwang Hoon Lee)

Aging of the skin is associated with delayed wound healing. This undesirable effect of aging is exacerbated by declining estrogen levels in postmenopausal women. Replacement of estrogen can increase collagen synthesis and keratinocyte migration to accelerate wound healing. Epithelial-mesenchymal transition (EMT) is a process in which epithelial cells gain a mesenchymal phenotype, leading to increased motility. Hence, the hypothesis that acceleration of keratinocyte migration by estrogen may be mediated by EMT was tested in this study. The goals of this study were to examine the relationship between estrogen-induced keratinocyte migration and EMT and to identify a novel protein associated with estrogen-induced EMT through stable isotope labeling by amino acids in cell culture (SILAC) analysis.

HaCaT immortalized human skin keratinocytes and primary human

keratinocytes (PHK) expressed only ER β . The expression of mesenchymal markers Slug, Twist, and vimentin was increased while the expression of the epithelial marker E-cadherin was decreased by treatment with 0.1, 1, 10, 100 nM estrogen for 48 h. The altered expression of these proteins was reversed following treatment with ICI, an estrogen receptor antagonist. The number of migrating cells was significantly increased in the presence of estrogen compared to control cells in wound scratch assay and transwell assay. Knockdown of Slug blocked estrogen-induced keratinocyte migration and reversed the changes in vimentin and E-cadherin induced by estrogen treatment.

SILAC-based mass spectrometry was performed on keratinocytes with or without estrogen treatment and 1085 proteins were identified. Thirty-two proteins were down-regulated and 60 proteins were up-regulated significantly. Among the 60 up-regulated proteins, 6 high-mobility group proteins were identified.

HMGB1 expression was increased after estrogen treatment, and the increased HMGB1 was reversed following treatment with ICI. The migration of keratinocytes was increased after treatment with recombinant HMGB1 protein and the estrogen-induced migration of keratinocytes was reversed by HMGB1 siRNA transfection. Knockdown of Slug in keratinocytes also resulted in a significant decrease in HMGB1.

These experiments demonstrate that estrogen contributes to keratinocyte

migration and that this activity may be mediated by the EMT process. Increased expression of HMGB1 may also be important in estrogen-induced keratinocyte migration and there may be a link between the EMT process and HMGB1.

Key words: estrogen, keratinocyte, migration, epithelial-mesenchymal transition (EMT), high mobility group B1 (HMGB1), stable isotope labeling by amino acids in cell culture (SILAC)

Role of estrogen in wound healing through regulation of epithelial-mesenchymal transition in human keratinocytes

Jung U Shin

*Department of Medicine
The Graduate School, Yonsei University*

(Directed by Professor Kwang Hoon Lee)

I. INTRODUCTION

Estrogen plays an important role in skin aging. Replacement of estrogen in postmenopausal women prevents skin aging by reducing skin wrinkling and increasing skin thickness and moisture content¹⁻⁵. Estrogen can also improve the delayed wound healing present in post-menopausal women^{6,7}. It is known that estrogen influences skin wound healing by modulating the inflammatory response^{8,9}, cytokine expression^{10,11}, and extracellular matrix deposition¹², accelerating re-epithelialization¹³ and stimulating angiogenesis¹⁴. However, the cellular and subcellular mechanisms of estrogen's action on keratinocyte migration are still poorly understood.

Epithelial-mesenchymal transition (EMT) is an important process in which epithelial cells lose their epithelial characteristics and acquire a

mesenchymal-like phenotype. This dramatic phenotypic change involves the loss of cell–cell adhesion and epithelial marker expression, as well as the loss of apical–basal polarity and the acquisition of a motile behavior and a profound reorganization of the cytoskeleton. EMT was first described in early embryogenesis and has recently been implicated in tissue repair, organ fibrosis, and cancer progression. In the skin, EMT has been implicated in skin morphogenesis^{15,16}, various skin cancers¹⁷⁻²⁰, wound healing²¹⁻²⁴, and skin fibrosis²⁵⁻²⁷. Recently, alterations of EMT-related molecules and migration ability in keratinocytes after various stimuli have been reported. For example, ultraviolet (UV) irradiation²⁸, epidermal growth factor (EGF)²⁹, transforming growth factor beta (TGF- β)^{28,30-32}, and tumor necrosis factor alpha (TNF- α)³² have been shown to alter the expression of EMT-inducing transcription factors and cell adhesion molecules.

Under the hypothesis that acceleration of keratinocyte migration by estrogen could be mediated by EMT, the ability of estrogen to induce the expression of Slug, Twist, and vimentin and to repress E-cadherin was examined. Stable isotope labeling by amino acids in cell culture (SILAC)-based mass spectrometry, a quantitative and differential proteomics technique, was performed to identify a novel protein associated with estrogen-induced EMT.

II. MATERIALS AND METHODS

1. Cell Culture

The spontaneously immortalized human skin keratinocyte cell line (HaCaT) was cultured in standard medium consisting of Dulbecco's modified Eagle medium (DMEM; Invitrogen; Burlington, ON, Canada) containing 10% fetal bovine serum (FBS; Invitrogen) and 1% antibiotic mixture (Gibco; S. Giuliano Milanese, Italy) at 37°C under 5% CO₂. When the cells reached 80% confluence, they were subcultured into new culture plates for continuous propagation and transferred to multi-well culture plates for experimental treatments.

2. Treatments

A. Estrogen

Prior to treatment with 17β-estradiol (E2) (Sigma-Aldrich; St. Louis, MO, USA), HaCaT cells were serum-starved overnight followed by stimulation with 0.1, 1, 10, 100, and 1,000 nM E2 dissolved in 100% ethanol for indicated times. All treatments were performed in duplicate or triplicate in each experiment.

The cells were seeded at 4×10^5 cells/well in six-well plates in DMEM/FBS and incubated for 24 h. Subsequently, the medium was removed and replaced with phenol red-free DMEM containing 10% charcoal-stripped

FBS and E2 or the same volume of ethanol as a vehicle control. To prepare charcoal-stripped serum, FBS was incubated with activated charcoal (10 mg/ml) for 2 h at 37°C. The serum was then centrifuged and the supernatant was passed through a 0.22- μ m filter (Millipore; Molsheim, France). Cells were pre-incubated for 1 h with the estrogen receptor antagonist, ICI (Tocris; Ballwin, MO, USA) or the G protein-coupled estrogen receptor-1, G15 (GPER/GPR-30; Tocris) before E2 stimulation.

B. Recombinant high-mobility group B1 (HMGB1) protein

Prior to treatment with recombinant HMGB1 (Sigma; H-4652), HaCaT cells were serum-starved overnight followed by stimulation with 0.5 μ g/ml and 1 μ g/ml HMGB1. All treatments were performed in duplicate or triplicate in each experiment.

3. Immunofluorescence

HaCaT and T47D cells were fixed in 4% paraformaldehyde, permeabilized with 0.1% Tween 20 when necessary, and saturated with 5% normal goat serum. Cells were then incubated with mouse anti-estrogen receptor α (anti-ER α ; 1:100) or rabbit anti-estrogen receptor β (anti-ER β ; 1:100) primary antibodies (both from Abcam; Cambridge, MA, USA). For double-labeling experiments, fluorescein isothiocyanate (FITC)-conjugated anti-mouse (1:250; Abcam) and Texas Red-conjugated anti-rabbit (1:250;

Abcam) secondary antibodies were used. Nuclei were then stained with 1 $\mu\text{g/ml}$ -diamidino-2-phenylindole (DAPI).

4. Cell viability assay

A 3-[4,5-dimethylthiazol-2-yl]-2,5 diphenyl tetrazolium bromide (MTT) assay was used to measure cell viability after different treatments. At each indicated time point, 10 μl of MTT (5 mg/ml; Sigma-Aldrich) was added to each well of a 96-well plate containing treated cells, and incubated for 4 h. Following incubation, 250 μl of dimethyl sulfoxide (DMSO) was added to dissolve the purple crystals, which are the products of the MTT substrate. After a 30-min incubation, the absorbance was measured on a plate reader at 570 nm.

5. Semi-quantitative and quantitative real-time polymerase chain reaction (RT-PCR)

Total RNA was extracted with the RNeasy Plus Mini Kit (Qiagen; Hilden, Germany) according to the manufacturer's instructions. cDNA was synthesized using the Transcriptor First Strand cDNA synthesis kit (Roche Applied Science; Mannheim, Germany) from 1 μg of total RNA.

The semi-quantitative PCR was performed with AccuPower[®] PCR PreMix (Bioneer, Seoul, Korea). The endogenous mRNA expression levels of ER α and ER β were confirmed with following oligonucleotide primers, with each

oligonucleotide sequence shown in 5' to 3' orientation (ER α forward primer: ATTATGGAGTCTGGTCCTGT, ER α reverse primer: CGGTCTTTTCGTATCCCACC, ER β forward primer: CCTCCTATGTAGACAGCCAC, ER β reverse primer: TGAGCATCCCTCTTTGAACC, *GAPDH* forward primer: AGAGCCTGGTGGAAAAGCTG, *GAPDH* reverse primer: AGCTCACCCCTACAGGATACC). The PCR amplification included 35 cycles of denaturation at 95°C for 1 min, annealing at 55°C for 1 min, and extension at 72°C for 1 min. The PCR products were electrophoresed on 1% agarose gels containing 10 μ g/ml EtBr and visualized with a CCD camera using UV light.

The quantitative RT-PCR was conducted in triplicate using TaqMan master mix (Applied Biosystems; Foster City, CA, USA) on the Real-Time PCR System (Applied Biosystems) using TaqMan assays (Applied Biosystems). The mRNA expression levels of Slug (assay ID: Hs00950344-A1), Twist (assay ID: Hs00361186-A1), Vimentin (assay ID: Hs00185584-A1), E-cadherin (assay ID: Hs01023894-A1), and *HMGB1* (assay ID: Hs01590761-g1) were normalized to that of the glyceraldehyde-3-phosphate dehydrogenase (*GAPDH*) (assay ID: Hs02758991-g1) housekeeping gene. Relative quantification was performed using Applied Biosystems 7500 software v2.0.1.

6. Immunoblot analysis

Cells were harvested in lysis buffer (1% Triton-X, 0.1% SDS, 0.5% sodium deoxycholate) with a protease inhibitor cocktail (Roche Diagnostics; Manheim, Germany), and protein concentrations were determined by using the Bradford protein assay (Bio-Rad Laboratories, Inc., Hercules, CA, USA). Proteins were separated by SDS-polyacrylamide gel electrophoresis (PAGE) (10% gel) and transferred to nitrocellulose membranes, which were blocked for 1 h with 5% skim milk in Tris-buffered saline containing Tween 20 (TBST) and incubated overnight at 4°C with the rabbit anti-human E-cadherin antibody (1:500), human Slug antibody (1:1,000), human Vimentin antibody (1:1,000), human HMGB1 antibody (1:1,000), human ER α antibody (1:1,000), and ER β antibody (1:1,000), all from Abcam. The primary antibodies were detected with horseradish peroxidase (HRP)-conjugated secondary antibodies (goat anti-mouse or rabbit; 1:2,000; Santa Cruz Biotechnology) and chemiluminescent luminol (Las 4000 mini; Fuji; Tokyo, Japan). Immunocomplexes were detected using an enhanced horseradish peroxidase/luminol chemiluminescence system (ECL Plus; Amersham International plc; Little Chalfont, UK). Immunoblot signals were quantified using a computer imaging program (GelScope; Imageline Inc.; Gardena, CA, USA).

7. Scratch assay

To examine whether estrogen or HMGB1 could stimulate keratinocyte migration, scratch assays were performed. Cells were grown to confluence and formed a monolayer covering the surface of the entire plate. Cells were kept in medium with appropriate treatments for 24 h prior to scratching. A linear scratch (~0.7-mm wide) was applied gently with a sterile pipette tip across the diameter of the well, and the cells were rinsed with phosphate-buffered saline (PBS) to remove debris. Fresh media for continued drug treatment were then added. For each well, at least six pictures were taken with a microscope at a magnification of 10× at four time points: 0, 24, 48, and 72 h after scratching.

8. Cell migration assay

Transwell assays were performed at 37°C using a 24-well Transwell containing a polycarbonate filter with 8-µm pores (Corning Costar; Action, MA, USA). Cells were incubated in E2 as previously described for 48 h and seeded in the upper well at a density of 50,000 cells per well. Lower wells contained 800 µl complete media with 10% FBS. After 3, 6, or 12 h of incubation, the cells were fixed in 4% formaldehyde in PBS for 30 min and stained with hematoxylin at room temperature for 5 min. The upper side of the membrane was scraped using a cotton swab to remove cells that had attached but not migrated. The membrane was then mounted onto a microscope slide.

Migration was assessed by counting the number of migrated cells in three random microscope fields ($\times 100$).

9. SILAC

A. Stable heavy isotope labeling

DMEM containing stable heavy isotope-labeled [$^{13}\text{C}_6$]-Lys, [$^{13}\text{C}_6$]-Arg or light Lys, Arg was prepared according to the SILAC kit manual instructions (http://tools.invitrogen.com/content/sfs/manuals/silac_man.pdf). HaCaT cells were serially subcultured for 6 doublings to obtain greater than 99% incorporation of the isotope-labeled Lys and Arg into proteins. The cells were plated in 10-cm dishes and designated as a light DMEM group and a heavy DMEM treated by E2 group, respectively. Based on previous studies, 100 nM E2 was treated on HaCaT cells for 24 h and the cells were harvested in lysis buffer (1% Triton-X, 0.1% SDS, 0.5% sodium deoxycholate) with a protease inhibitor cocktail (Roche Diagnostics; Mannheim, Germany). Cell lysates with heavy and light Lys and Arg were mixed at a 1:1 ratio. Protein concentrations were determined by using the Bradford protein assay (Bio-Rad Laboratories, Inc., Hercules, CA, USA). The general experimental procedure is shown in Figure 1.

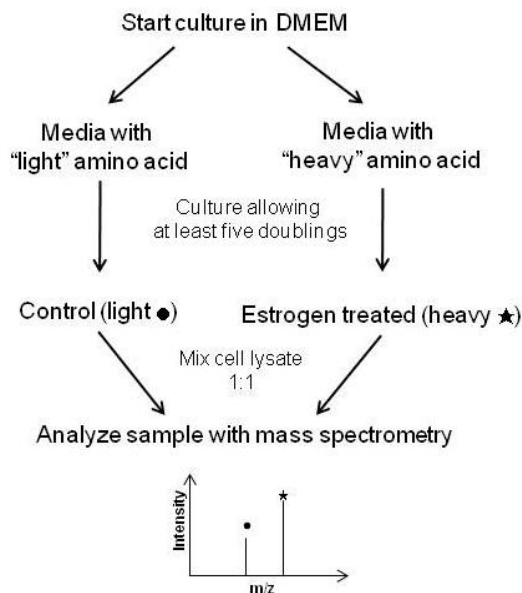


Figure 1. Schematic diagram of general experimental procedure of SILAC.

Cells were SILAC-labeled using heavy [$^{13}\text{C}_6$]-Lys, [$^{13}\text{C}_6$]-Arg or light Lys, Arg. Light- and heavy-labeled cells were mixed in equal proportions. Proteins were digested using trypsin and peptide mixtures, and were analyzed by liquid chromatography tandem mass spectrometry (LC-MS/MS).

B. Protein preparation

The protein concentration was determined using the BCA method (Bio-Rad). One hundred micrograms of protein with 10 mM dithiothreitol (DTT) was incubated at 56°C for 1 h. After cooling to room temperature, the protein was alkylated by 50 mM iodacetamide (IAM) in a dark room for 45 min. Excess IAM was removed using 40 mM DTT at room temperature. The

sample was further diluted 5-fold with 25 mM NH_4HCO_3 , and 1% trypsin was sequentially added to digest the protein for 12 h and 6 h at 37°C, respectively. The debris was removed by centrifugation for 10 min at 13,000 $\times g$. The supernatant was stored at -80°C for mass spectrometry (MS) analysis.

C. Materials

Formic acid, ammonium bicarbonate, urea, DTT, and iodoacetic acid (IAA) were purchased from Sigma-Aldrich. Sequencing-grade modified trypsin was purchased from Promega (Madison; WI, USA). High-performance liquid chromatography (HPLC)-grade acetonitrile was purchased from Burdick and Jackson (Muskegon; MI, USA). Water was purified using a Milli Q system (Millipore; Molsheim, France).

D. Sample preparation

The proteins from keratocytes were denatured in 8 M urea and reduced with 10 mM DTT at 37°C for 30 min. IAA was added to a final concentration of 20 mM, and the resulting mixture was incubated at 37°C in the dark for 30 min. For removal of excess reagent, the sample was subjected to a Vivaspin column with a 5,000 molecular weight cut-off polyethersulfone (PES) membrane, and was washed with 100 mM of triethyl ammonium bicarbonate (TEAB) buffer. After protein quantitation, 100 μg of protein was dissolved in 100 mM of TEAB (pH 8.0) to a final concentration of 1 $\mu\text{g}/\mu\text{l}$. To perform

protein digestion, trypsin (1:20 protease-to-protein ratio) was added, and the mixture was incubated overnight at 37°C. The sample was dissolved in 50 µl of water containing 0.1% formic acid for liquid chromatography coupled with tandem mass spectrometry (LC-MS/MS) analysis.

E. Two-dimensional (2D)-LC-MS/MS

The samples were analyzed using a 2D-LC-MS/MS system consisting of a nanoACQUITY Ultra Performance LC System (Waters; Milford, MA, USA) and a LTQ Orbitrap Elite mass spectrometer (Thermo Scientific; Hudson, NH, USA) equipped with a nano-electrospray source. A detailed description of 2D-LC-MS/MS analysis can be found in the literature³³. Briefly, a strong cation exchange (5 µm, 3 cm) column was placed just before the C18 trap column (internal diameter (id) 180 µm, length 20 mm, and particle size 5 µm; Waters). Peptide solutions were loaded in 9-µl aliquots for each run. Peptides were displaced from the strong cation exchange phase to the C18 phase by using a salt gradient that was introduced through an autosampler loop, and were then desalted for 10 min at a flow rate of 4 µl/min. Next, the trapped peptides were separated on a 200-mm microcapillary column made in-house consisting of C18 (Aqua; particle size 3 µm) packed into 100-µm silica tubing with an orifice id of 5 µm.

An eleven-step salt gradient was performed using 9 µl of sample aliquots, 3 µl of 25, 50, 100, 250, and 500 mM ammonium acetate (0.1% formic acid in

5% acetonitrile (ACN)) and 4, 5, 9, and additional 9 μ l and 500 mM ACN (0.1% formic acid in 30% ACN). The mobile phases, A and B, were composed of 0 and 100% ACN, respectively, and each contained 0.1% formic acid. The LC gradient began with 5% B for 1 min and was ramped to 20% B over 5 min, to 50% B over 90 min, to 95% B over 1 min, and remained at 95% B over 13 min and at 5% B for another 5 min at a flow rate of 0.4 μ l/min. The column was re-equilibrated with 5% B for 15 min before the next run. The voltage applied to produce an electrospray was 2.0 kV. During the chromatographic separation, the LTQ Orbitrap Elite was operated in data-dependent mode. The MS data were acquired using the following parameters: ten data-dependent collision-induced dissociation (CID) MS/MS scans per full scan; CID scans were acquired in linear trap quadrupole (LTQ) with four-microscan averaging; full scans were acquired in FT (Orbitrap) at 60,000 resolution; 35% normalized collision energy (NCE) in CID; \pm 1 Da isolation window. Previously fragmented ions were excluded for 60 s.

F. Protein identification and quantification

MS/MS spectra were analyzed using the following software analysis protocols with the IPI rat database (IPI.rat. 7.26.2012). The reversed sequences of all proteins were appended into the database for calculation of the false discovery rate (FDR). ProLucid³⁴ was used to identify the peptides with a precursor mass error of 25 ppm and a fragment ion mass error of 600

ppm. Trypsin was selected as the enzyme, with three potential missed cleavages. Heavy isotope-labeled lysine (+6) and arginine (+10) residues by using the labeling reagent and carbamidomethylation at cysteine were chosen as static modifications. Oxidation at methionine was chosen as variable modification. The output data files were filtered and sorted to compose the protein list using DTASelect³⁵ (The Scripps Research Institute; La Jolla, CA, USA) with two and more peptide assignments for a protein identification and a false positive rate less than 1%.

A quantitative analysis was conducted using Census in the IP2 pipeline (Integrated Proteomics; USA). The light to heavy ratios of proteins were calculated as the averages of all constituent peptides in the identified protein.

10. Transfection of small interfering RNAs

Small interfering RNAs (siRNAs) specific to Slug and HMGB1 (on-TARGETplus SMARTpool) were obtained from Dharmacon (Lafayette, CO, USA). Transient transfections of HaCaT cells were performed according to the DharmaFECT general transfection protocol for a 6-well plate format. Briefly, 1.5×10^5 cells per well of a 6-well dish were seeded and incubated in antibiotic-free medium containing fetal bovine serum at 37°C for 24 h prior to siRNA transfection. In separate polystyrene tubes, 10 nM siRNA (final concentration) and 2 μ l DharmaFECT 1 reagent (Dharmacon) were mixed in serum- and antibiotic-free media and incubated at room temperature for 5 min.

The siRNA-containing medium was added to the tube containing the DharmaFECT 1 reagent and these contents were mixed and incubated for 20 min at room temperature. Serum-containing media was added to the mix and the cells were incubated in this siRNA-containing media for 24–48 h at 37°C in a humidified incubator with 5% CO₂.

11. Statistical analyses

All assays were repeated at least three times in duplicate or triplicate, and the data are presented as the mean \pm SD. The results obtained were analyzed by using paired Student's t-tests and one-way analysis of variance (ANOVA). Deviations were considered statistically significant when $p < 0.05$.

III. RESULTS

1. Expression of estrogen receptors α and β in HaCaT cells

The expression of estrogen receptors (ERs) α and β in HaCaT cells and primary human keratinocytes (PHK) was analyzed by immunofluorescence. T47D breast cancer cells were used as a positive control for ERs α and β . Whereas T47D cells expressed both ER α and ER β , HaCaT cells and PHK expressed only ER β (Figure 2a). To further confirm these results, semi-quantitative RT-PCR (Figure 2b) and western blot analysis (Figure 2c) were performed, and the results were confirmed. It is already known that ER α and ER β both bind E2 with nearly equal affinity³⁶. Therefore, further experiments were performed using ER β -expressing HaCaT cells to evaluate the effects of estrogen on keratinocytes.

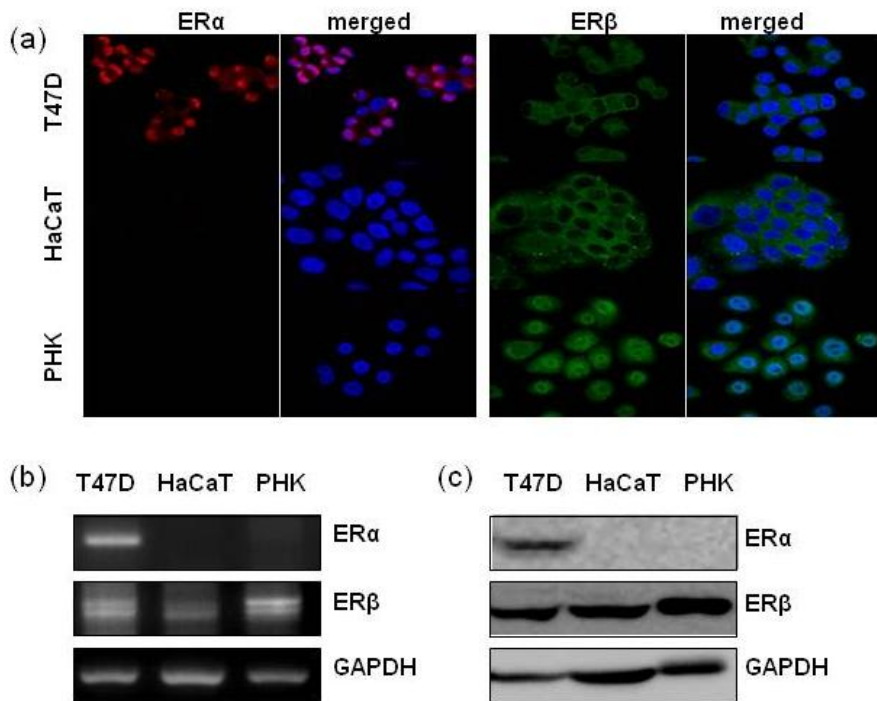


Figure 2. Expression of estrogen receptors (ERs) in HaCaT cells and primary human keratinocytes (PHK). (a) Immunofluorescence staining of ER α and ER β in HaCaT cells and PHK. T47D cells were used as a positive control for ER expression; T47D cells express both ER α and ER β , whereas HaCaT cells and PHK express only ER β . (b) Semi-quantitative RT-PCR analysis of ER α and ER β in HaCaT cells and PHK. Both HaCaT cells and PHK only expressed ER β at the mRNA level. (c) Western blot analysis of ER α and ER β in HaCaT cells and PHK. Both HaCaT cells and PHK only expressed ER β at the protein level.

2. Effect of E2 on the viability of HaCaT cells

The viability of HaCaT cells was measured using an MTT assay. While E2 had no effect on cell viability at lower concentrations, there was a statistically significant reduction in cell viability after treatment with 1000 nM E2 ($p < 0.0001$, Figure 3).

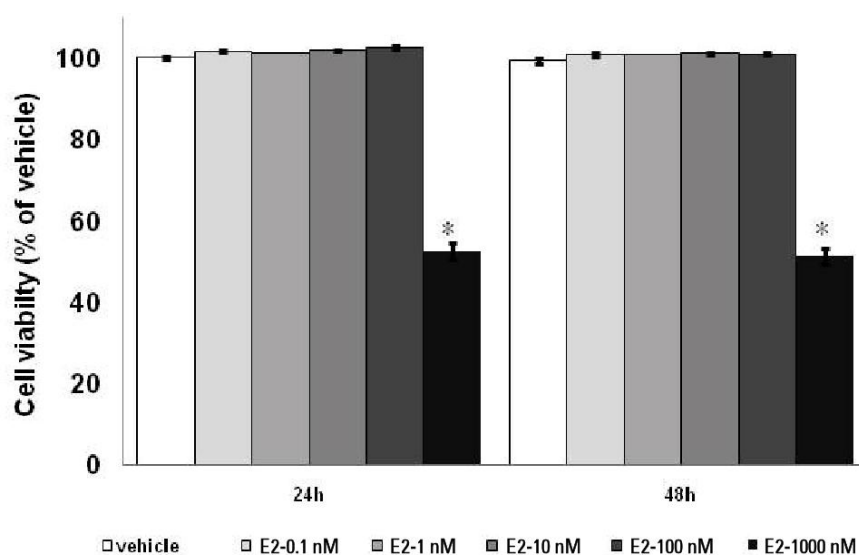
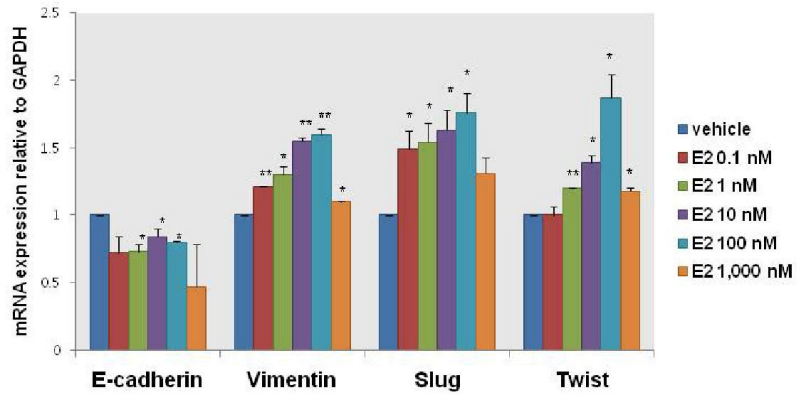


Figure 3. Cell viability as determined using an MTT assay. HaCaT cells were treated with 0.1, 1, 10, 100, or 1000 nM E2 for the indicated time points. There were no significant changes in cell viability after treatment of 0.1, 1, 10, and 100 nM E2. However, after treatment with 1000 nM E2, cell viability was significantly reduced ($*p < 0.0001$).

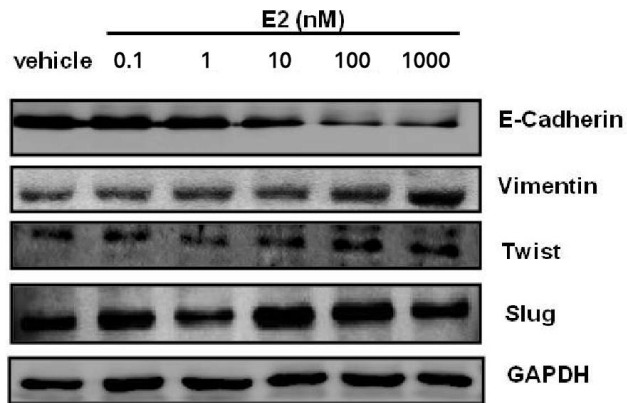
3. Estrogen modulates EMT-related molecules in HaCaT cells

HaCaT cells were treated with 0.1, 1, 10, 100 nM, or 1000 nM E2. The stimulatory effect of E2 on Slug and Twist mRNA expression was determined by quantitative RT-PCR (qRT-PCR). Both Slug and Twist mRNA levels were increased after 48 h treatment with 0.1, 1, 10, and 100 nM E2, while 1000 nM estradiol did not increase Slug and Twist mRNA levels (Figure 4a). Because alterations of E-cadherin (decrease) and vimentin (increase) have been reported to be crucial markers for the EMT process, the mRNA levels of E-cadherin and vimentin were measured after E2 treatment. After 48 h treatment of E2, the mRNA level of E-cadherin was reduced and that of vimentin was increased (Figure 4a). The alteration of these molecules after estrogen treatment was also confirmed by western blot analysis (Figure 4b) and direct immunofluorescence (Figure 4c).

(a)



(b)



(c)

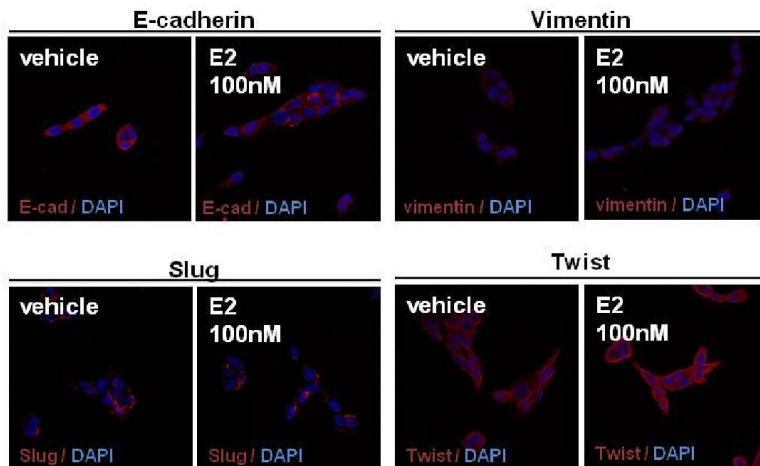


Figure 4. Up-regulated Slug, Twist, and vimentin and down-regulated E-cadherin in HaCaT cells after treatment with E2. (a) Real-time PCR analysis of E-cadherin, vimentin, Slug, and Twist in HaCaT cells after treatment with 0.1, 1, 10, 100 and 1,000 nM E2 for 48 h. (b) Western blot analysis of E-cadherin, vimentin, Slug, and Twist in HaCaT cells ($*p < 0.05$, $**p < 0.01$). (c) Increased expression of Slug, Twist, and vimentin (red immunofluorescence staining) and decreased expression of E-cadherin (red) were noted after E2 (100 nM) treatment. Nuclei were stained with DAPI (blue).

4. Effects of estrogen on EMT-related molecules through the ER

The changes in EMT-related molecules were reversed following treatment with ICI, an estrogen receptor antagonist. However, G15, an antagonist of another estrogen-related receptor, GPR30, could not reverse the changes in EMT-related molecules (Figure 5). Therefore, these data indicate that estrogen regulates EMT-related molecules through ERs and not GPR30.

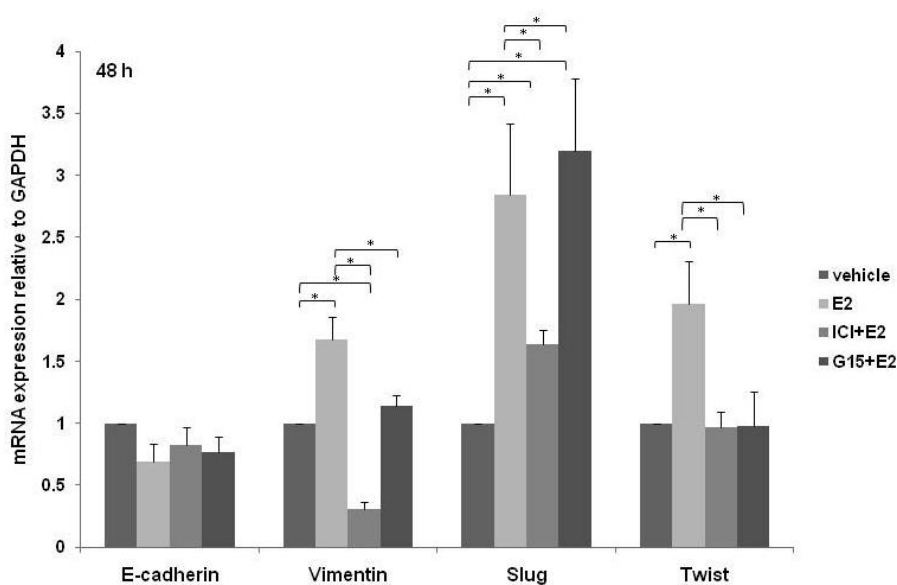


Figure 5. Estrogen receptor (ER) mediates E2-induced E-cadherin, vimentin, Slug, and Twist expression in HaCaT cells. Serum-starved cells were pretreated for 1 h with ICI or G15 and then treated with 100 nM E2 for 48 h. RNA levels were analyzed and quantified by qRT-PCR. Inhibition of ER but not GPR30 blocked the E2-induced Slug, Twist, and vimentin mRNA expression (* $p < 0.05$).

5. Estrogen stimulates the migration of HaCaT cells

To investigate whether estrogen can alter the rate of cell migration, scratch and Transwell assays were performed. After scratching a confluent monolayer of HaCaT cells with a P200 pipette tip and completely removing debris by washing, cells were treated with 0.1, 1, 10, or 100 nM E2. Images of the same field were captured at 0, 24, 48, and 72 h after scratching (Figure 6a). Transwell assay was performed with 8- μ m polycarbonate filters (Figure 6b). In the presence of estrogen, the numbers of migrating cells were significantly increased as compared with those of control cells.

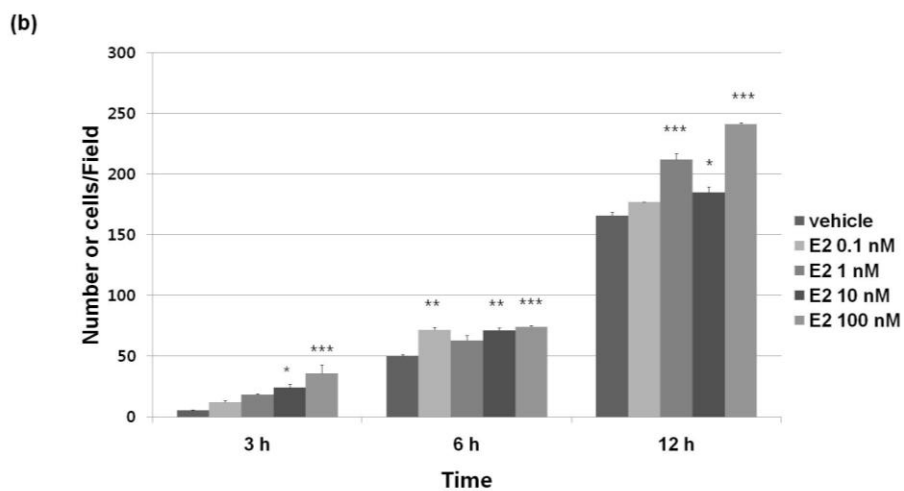
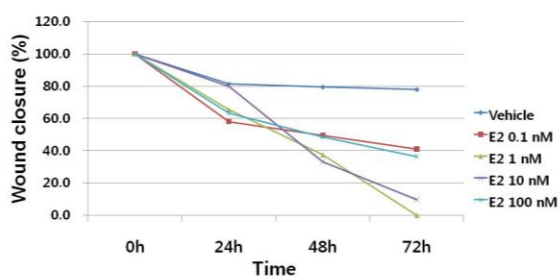
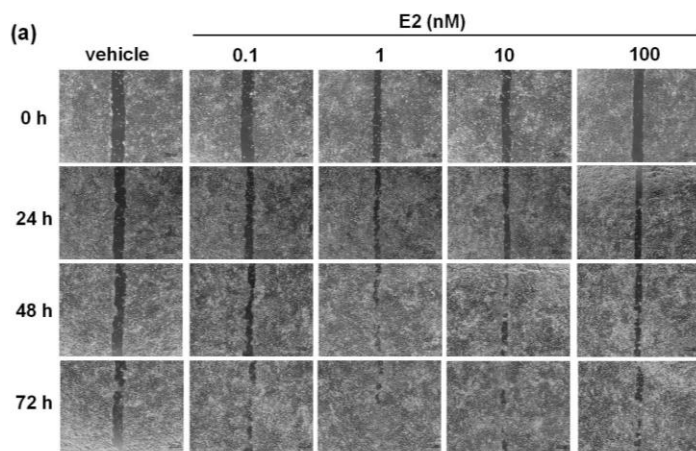
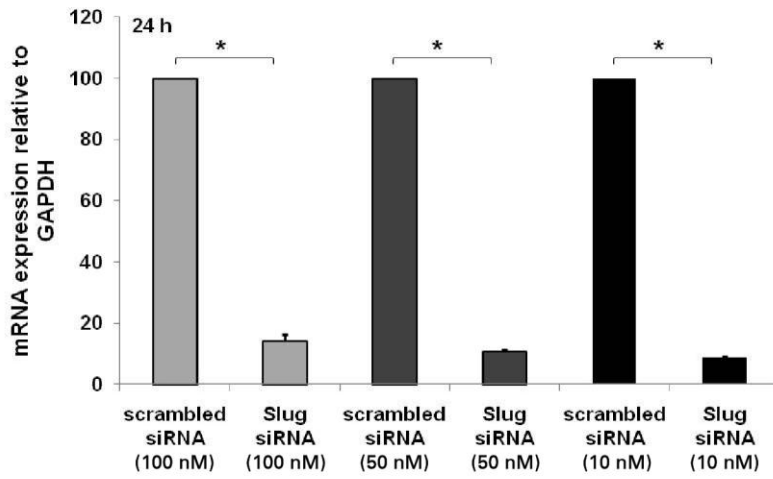


Figure 6. Estrogen promotes the migration of HaCaT cells. (a) HaCaT cell migration with the addition of E2 at different time points after scrape wounding of the keratinocyte monolayer. E2 stimulated the migration of HaCaT cells over the wound area. (b) The number of cells that migrated through the 8- μm pore-size membrane of a Transwell insert is shown ($*p < 0.05$, $** p < 0.01$, $***p < 0.001$). After 3, 6, and 12 h of incubation, 100 nM estrogen showed the most remarkable increase in migration.

6. Slug knockdown impairs the migration of HaCaT cells

To determine whether Slug is involved in the migration of HaCaT cells, cells were transfected with three concentrations of Slug siRNA before E2 (100 nM) stimulation. After 24 h transfection, the mRNA level of Slug was significantly decreased by transfection with 100, 50, or 10 nM siRNA by 86%, 90%, and 91%, respectively ($p < 0.05$), as compared with the scrambled siRNA groups (Figure 7a). Using a scratch assay, the migration of HaCaT cells was markedly inhibited by transfection with Slug siRNA as compared to cells transfected with scrambled siRNA (Figure 7b).

(a)



(b)

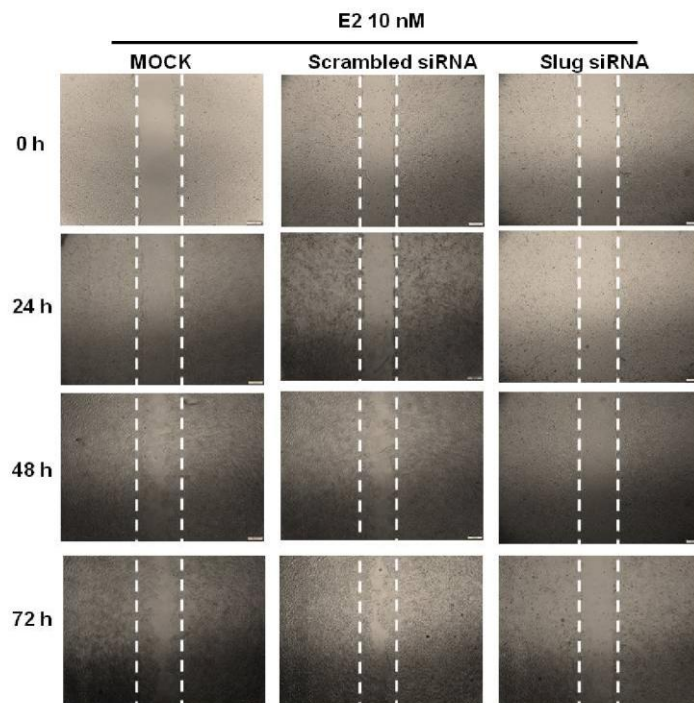


Figure 7. Knockdown of Slug inhibits the migration of HaCaT cells. (a) The expression of Slug was down-regulated by Slug siRNA transfection. Slug mRNA levels were determined by qRT-PCR. ($*p < 0.05$). (b) The migration of HaCaT cells was inhibited significantly, corresponding to the down-regulation of Slug.

7. Slug knockdown modulates E-cadherin and vimentin expression

To determine how Slug is involved in the migration of HaCaT cells, cells were transfected with Slug siRNA before E2 (100 nM) stimulation. The mRNA levels of E-cadherin and vimentin were measured after Slug siRNA transfection. After 48 h transfection, the mRNA level of E-cadherin was increased while that of vimentin was reduced (Figure 8).

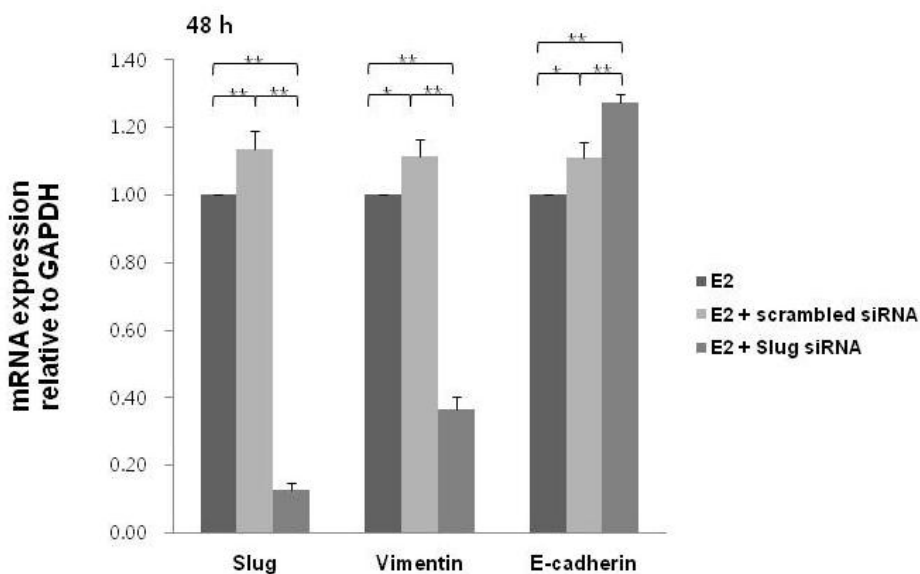


Figure 8. Up-regulated vimentin and down-regulated E-cadherin after Slug siRNA transfection. The vimentin level was decreased and the E-cadherin level was increased at 48 h post-transfection of Slug siRNA ($*p < 0.05$, $**p < 0.01$).

8. Proteome alterations following E2 treatment as revealed by SILAC

To quantitate protein expression changes, SILAC-based proteome analysis was performed to determine differences between the HaCaT cells before and after E2 treatment. Quantification of 1085 proteins was achieved through nanoLC/electrospray ionization (ESI)-MS/MS analysis. Quantification was based on the peak area of precursor ions of more than two peptides including one unique peptide. Ratios were averaged and proteins with ratio values with $p < 0.05$ in normal distribution were defined as significantly regulated. Ninety two proteins (32 down-regulated and 60 up-regulated) showing an up/down modulation (Table 1 and 2) were selected for further analysis.

Among the 60 up-regulated proteins, high mobility group proteins were frequently found. A total of 6 up-regulated high mobility group proteins are listed in Table 3. Among these 6 proteins, high mobility group protein B1 (HMGB1) has been reported to be associated with aging and the wound healing process. Figure 9 shows extracted ion chromatograms of three HMGB1-related peptides: K.KLGEMWNNTAADDKQPYEKK.A, K.GKPDAAKKGVVK.A, and K.IKGEHPGLSIGDVAKK.L. All of these peptides showed higher peak areas in E2-treated HaCaT cells as compared to control cells. Therefore, further evaluation of the role of HMGB1 in the estrogen-induced EMT process was performed.

Table 1. Thirty-two down-regulated ($p < 0.05$) proteins after 17 β -estradiol treatment in HaCaT cells.

Number	Average ratio	CV	Peptide count	Standard deviation	Gene	Protein
IPI00013068	0.65	29.2	2	0.19	EIF3E	Eukaryotic translation initiation factor 3 subunit E
IPI01011969	0.67	3	2	0.02	NUP88	cDNA FLJ58372, highly similar to Nuclear pore complex protein Nup88
IPI00334159	0.71	7	2	0.05	VBP1	von Hippel-Lindau binding protein 1, isoform CRA_b
IPI00942032	0.72	29.2	4	0.21	AGR2	Anterior gradient protein 2 homolog
IPI00550239	0.73	13.7	2	0.1	H1F0	Histone H1.0
IPI00181717	0.73	11	2	0.08	MAT2B	Isoform 2 of Methionine adenosyltransferase 2 subunit beta
IPI00015361	0.74	23	2	0.17	PFDN5	Prefoldin subunit 5
IPI00963899	0.74	23	4	0.17	HMGCS1	cDNA FLJ38173 fis, clone FCBBF1000053, highly similar to HYDROXYMETHYLGLUTARYL-COA SYNTHASE, CYTOPLASMIC
IPI00008164	0.74	10.8	3	0.08	PREP	Prolyl endopeptidase
IPI00604497	0.74	28.4	2	0.21	HERC4	HERC4 protein
IPI00792971	0.75	12	2	0.09	IDH3A	Isoform 2 of Isocitrate dehydrogenase [NAD] subunit alpha, mitochondrial
IPI00002879	0.77	10.4	2	0.08	C14orf169	Isoform 1 of Lysine-specific demethylase NO66
IPI00032406	0.8	15	2	0.12	DNAJA2	DnaJ homolog subfamily A member 2
IPI00647395	0.8	15	2	0.12	TSNAX	Disrupted in schizophrenia 1 isoform 54
IPI00025796	0.8	0	2	0	NDUFS3	NADH dehydrogenase [ubiquinone] iron-sulfur protein 3, mitochondrial
IPI00854869	0.81	16	5	0.13	TNS3	Isoform 2 of Tensin-3
IPI00220668	0.81	22.2	2	0.18	SHMT1	Isoform 2 of Serine hydroxymethyltransferase, cytosolic
IPI00925520	0.81	25.9	2	0.21	PFKL	Similar to Phosphofructokinase

IPI00024254	0.82	17.1	7	0.14	IFIT3	Interferon-induced protein with tetratricopeptide repeats 3
IPI00413785	0.82	9.8	5	0.08	FGD3	Isoform 2 of FYVE, RhoGEF and PH domain-containing protein 3
IPI00007058	0.82	15.9	2	0.13	CORO1B	Coronin-1B
IPI00966084	0.83	9.6	2	0.08	COPS4	Uncharacterized protein
IPI00964070	0.84	8.3	2	0.07	ANXA3	Uncharacterized protein
IPI00976539	0.84	22.6	3	0.19	TTC1	19 kDa protein
IPI00103027	0.84	13.1	2	0.11	SPATS2L	Isoform 2 of SPATS2-like protein
IPI00028931	0.84	16.7	2	0.14	DSG2	Desmoglein-2
IPI00026781	0.85	2.4	39	0.02	FASN	Fatty acid synthase
IPI00221222	0.85	21.2	8	0.18	SUB1	Activated RNA polymerase II transcriptional coactivator p15
IPI00291483	0.85	1.2	2	0.01	AKR1C3	Aldo-keto reductase family 1 member C3
IPI01012302	0.85	16.5	6	0.14	IFIT1	Uncharacterized protein
IPI00619903	0.85	14.1	3	0.12	UGGT1	Isoform 2 of UDP-glucose:glycoprotein glucosyltransferase 1
IPI00412752	0.85	7.1	2	0.06	STAT3	signal transducer and activator of transcription 3 isoform 3

Table 2. Sixty up-regulated ($p < 0.05$) proteins after 17 β -estradiol treatment in HaCaT cells

Number	Average ratio	CV	Peptide count	Standard deviation	Gene	Protein
IPI00026546	1.18	16.9	5	0.2	PAFAH1B2	Platelet-activating factor acetylhydrolase IB subunit beta
IPI00940656	1.18	5.1	11	0.06	ANP32A	P1 Uncharacterized protein
IPI00456049	1.18	4.2	2	0.05	ATP5H	Isoform 2 of ATP synthase subunit d, mitochondrial
IPI00180730	1.18	8.5	8	0.1	-	alpha 1
IPI01018954	1.18	23.7	6	0.28	HADHB	cDNA FLJ56214, highly similar to Trifunctional enzyme subunit beta, mitochondrial
IPI00925323	1.18	15.3	5	0.18	RPL14	60S ribosomal protein L14
IPI00793232	1.18	3.4	3	0.04	PNPO	cDNA FLJ59109, highly similar to Pyridoxine-5'-phosphate oxidase
IPI00021785	1.18	4.2	3	0.05	COX5B	Cytochrome c oxidase subunit 5B, mitochondrial
IPI00383539	1.18	10.2	11	0.12	CS	Citrate synthase
IPI00966243	1.18	0.8	2	0.01	CYB5B	Uncharacterized protein
IPI00006378	1.18	11.9	2	0.14	CCDC72	Coiled-coil domain-containing protein 72
IPI00304612	1.18	5.9	6	0.07	SNORD32A	;RPL13A;SNORD33;SNORD34 60S ribosomal protein L13a
IPI00306516	1.18	0.8	2	0.01	TIMM44	Mitochondrial import inner membrane translocase subunit TIM44
IPI00852712	1.18	10.2	2	0.12	SNORA56	;DKC1 Uncharacterized protein
IPI00555581	1.18	21.2	2	0.25	MCM5	Minichromosome maintenance deficient protein 5 variant (Fragment)
IPI00290043	1.18	22.0	2	0.26	ITGA3	Isoform 2 of Integrin alpha-3
IPI00953668	1.18	3.4	3	0.04	IGF2BP3	Uncharacterized protein
IPI00797738	1.19	11.8	4	0.14	COX6B1	Cytochrome c oxidase subunit 6B1
IPI00022145	1.19	9.2	5	0.11	NUCKS1	Isoform 1 of Nuclear ubiquitous casein and cyclin-dependent kinases substrate

IPI01012111	1.19	15.1	2	0.18	-	Similar to 60S ribosomal protein L29
IPI00374657	1.19	12.6	2	0.15	VAPA	Isoform 2 of Vesicle-associated membrane protein-associated protein A
IPI00155466	1.2	6.7	3	0.08	SUCLG2	Uncharacterized protein
IPI00985110	1.2	12.5	3	0.15	NSF	cDNA FLJ59316, highly similar to Vesicle-fusing ATPase
IPI00219350	1.2	3.3	2	0.04	MRPS11	Isoform 2 of 28S ribosomal protein S11, mitochondrial
IPI00218176	1.2	5.0	2	0.06	POFUT1	Isoform 2 of GDP-fucose protein O-fucosyltransferase 1
IPI00177716	1.21	5.8	3	0.07	HMGA1	Isoform HMG-Y of High mobility group protein HMG-I/HMG-Y
IPI01009955	1.21	3.3	3	0.04	BCAP31	B-cell receptor-associated protein 31 isoform a
IPI00021187	1.21	25.6	4	0.31	RUVBL1	Isoform 1 of RuvB-like 1
IPI00450235	1.21	16.5	3	0.2	YBX1	Nuclease sensitive element binding protein-1
IPI00337541	1.21	14.9	3	0.18	NNT	NAD(P) transhydrogenase, mitochondrial
IPI00829826	1.21	0.8	2	0.01	MED1	Isoform 1 of Mediator of RNA polymerase II transcription subunit 1
IPI00419258	1.22	4.9	16	0.06	HMGB1	High mobility group protein B1
IPI00017510	1.22	2.5	3	0.03	MT	-CO2 Cytochrome c oxidase subunit 2
IPI00980468	1.22	8.2	3	0.1	MAOA	cDNA FLJ61220, highly similar to Amine oxidase (flavin-containing) A
IPI00646144	1.22	13.1	3	0.16	ATAD3A	ATPase family AAA domain-containing protein 3A isoform 3
IPI00549569	1.22	5.7	2	0.07	ISYNA1	Isoform 1 of Inositol-3-phosphate synthase 1
IPI01015591	1.22	18.9	2	0.23	DHX15	Uncharacterized protein
IPI00217950	1.23	3.3	3	0.04	HMGN2	Non-histone chromosomal protein HMG-17
IPI00027462	1.24	1.6	2	0.02	S100A9	Protein S100-A9
IPI00219097	1.24	11.3	9	0.14	HMGB2	High mobility group protein B2
IPI00171277	1.24	4.0	2	0.05	HMGN3	Isoform 2 of High mobility group nucleosome-binding domain-containing protein 3

IPI00847300	1.24	7.3	2	0.09	-	selective channel protein 1
IPI00646889	1.24	5.6	2	0.07	C10orf58	;C10orf57 Uncharacterized protein
IPI00215920	1.25	3.2	2	0.04	ARF6	ADP-ribosylation factor 6
IPI00456695	1.25	2.4	2	0.03	PSMD1	Isoform 2 of 26S proteasome non-ATPase regulatory subunit 1
IPI01012315	1.25	10.4	3	0.13	PTGFRN	protein (Fragment)
IPI00179700	1.26	5.6	3	0.07	HMGA1	Isoform HMG-I of High mobility group protein HMG-I/HMG-Y
IPI00384967	1.26	12.7	8	0.16	ALDH1A3	Putative uncharacterized protein DKFZp686G1675 (Fragment)
IPI00012442	1.26	18.3	6	0.23	G3BP1	Ras GTPase-activating protein-binding protein 1
IPI00216919	1.26	12.7	2	0.16	YAP1	Isoform 1 of Yorkie homolog
IPI00003927	1.27	25.2	2	0.32	PPID	Peptidyl-prolyl cis-trans isomerase D
IPI00871988	1.28	10.2	2	0.13	SFXN3	cDNA FLJ58980, highly similar to Sideroflexin-3
IPI00973950	1.28	18.0	2	0.23	AK3	;AK4 Uncharacterized protein
IPI00006865	1.3	17.7	3	0.23	SEC22B	Vesicle-trafficking protein SEC22b
IPI00305282	1.3	25.4	4	0.33	RAD50	RAD50 protein
IPI00646721	1.35	20.7	3	0.28	USP7	Ubiquitin carboxyl-terminal hydrolase
IPI00154975	1.37	16.1	2	0.22	DNAJC9	DnaJ homolog subfamily C member 9
IPI00893815	1.46	15.1	2	0.22	NIPSNAP1	Protein
IPI00065063	1.57	15.3	2	0.24	DHRS1	Dehydrogenase/reductase SDR family member 1
IPI00019903	3.59	2.2	2	0.08	TACO1	Translational activator of cytochrome c oxidase I

Table 3. Six up-regulated (protein ratio > 1.2) high mobility group proteins after 17 β -estradiol treatment in HaCaT cells

Number	Average ratio	CV	Peptide count	Standard deviation	Gene	Protein
IPI00177716	1.21	5.8	3	0.07	HMGA1	Isoform HMG-Y of High mobility group protein HMG-I/HMG-Y
IPI00419258	1.22	4.9	16	0.06	HMGB1	High mobility group protein B1
IPI00217950	1.23	3.3	3	0.04	HMGN2	Non-histone chromosomal protein HMG-17
IPI00219097	1.24	11.3	9	0.14	HMGB2	High mobility group protein B2
IPI00171277	1.24	4	2	0.05	HMGN3	Isoform 2 of High mobility group nucleosome-binding domain-containing protein 3
IPI00179700	1.26	5.6	3	0.07	HMGA1	Isoform HMG-I of High mobility group protein HMG-I/HMG-Y

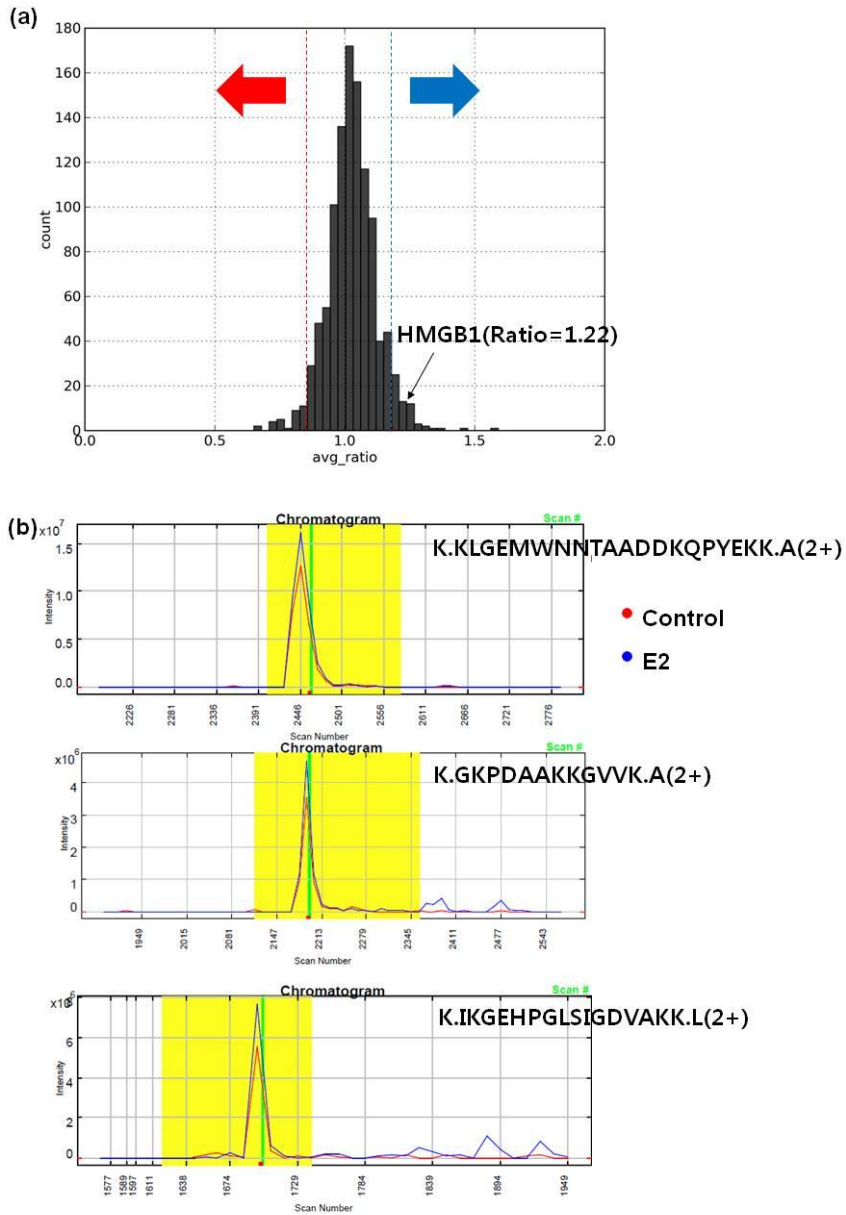


Figure 9. SILAC protein identification. (a) Distribution of total protein ratio. In this distribution, proteins with ratio values with $p < 0.05$ in normal distribution were defined as significantly regulated. HMGB1 was located

in the up-regulated proteins area with a ratio of 1.22. (b) Extracted ion chromatogram of the HMGB1-related peptides, K.KLGEMWNNTAADDKQPYEKK.A, K.GKPDAAKKGVVK.A, and K.IKGEHPGLSIGDVAKK.L.

9. Estrogen increases HMGB1 expression via the estrogen receptor

qRT-PCR and western blot analysis were performed to confirm the elevation of HMGB1 expression after stimulation with estrogen in HaCaT cells. Treatment with 0.1, 1, 10, and 100 nM E2 increased HMGB1 at the RNA and protein levels (Figure 10a and 10b). After stimulation with 1000 nM E2, HMGB1 expression was not increased, which can be explained by the cell toxicity of high-dose E2 as discussed above in section 2. Nuclear HMGB1 was elevated after stimulation with E2, but cytoplasmic HMGB1 was not elevated. HMGB1 in culture supernatants was detected by western blotting, and the release of HMGB1 was increased by E2 treatment after 48 h (Figure 10c). Increased levels of both HMGB1 and Slug were reversed with ICI treatment but not with G15 treatment (Figure 10d). Therefore, these data indicate that induction of Slug and HMGB1 by estrogen occurs through the estrogen receptor and not GPR30.

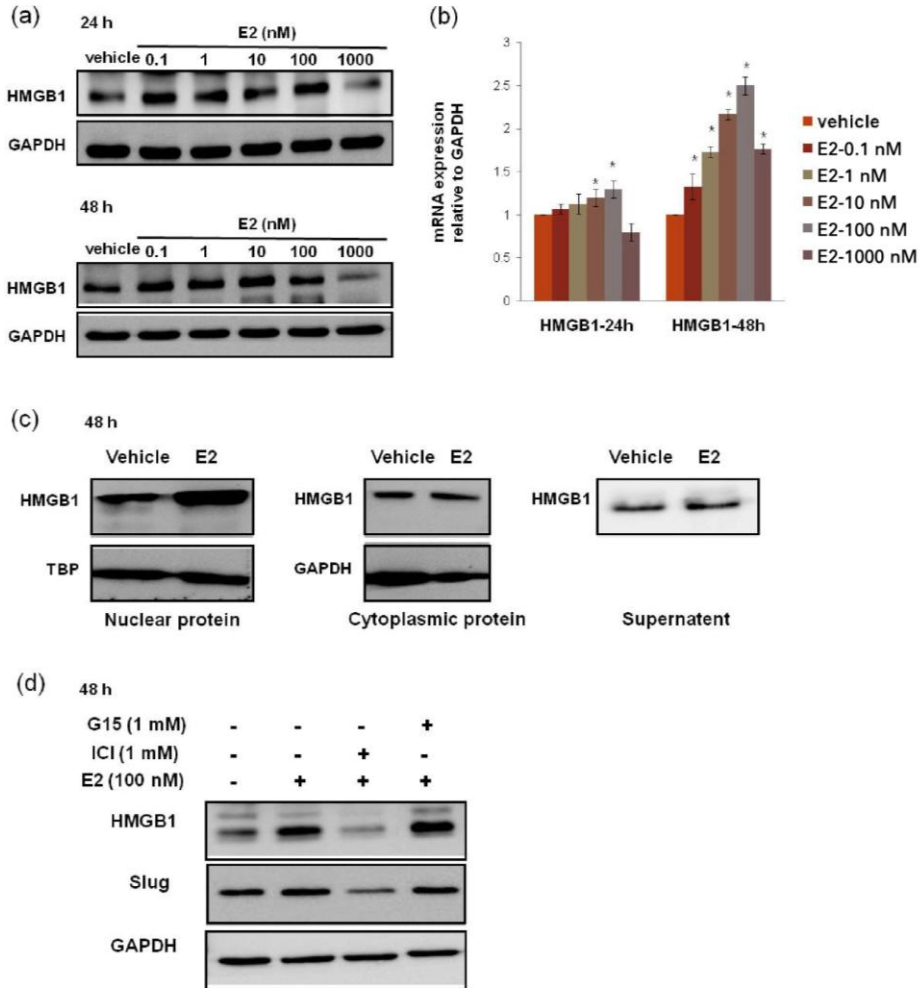


Figure 10. E2 induces HMGB1 expression. Serum-starved HaCaT cells were treated with 0.1, 1, 10, 100, and 1000 nM E2 for the indicated times. Protein and mRNA levels were measured by western blot (a) and qRT-PCR (b) ($*p < 0.05$). (c) Western blot analysis to detect HMGB1 levels in nuclear, cytoplasmic, and culture supernatant protein extracts. Nuclear HMGB1 and secreted HMGB1 were increased after E2 treatment. (d) Estrogen receptor

(ER)-mediated E2-induced HMGB1 expression. Cells were pretreated with ICI and G15 as described in the legend for Figure 5. HMGB1 protein levels were analyzed by western blot analysis. Inhibition of ER but not GPR30 blocked E2-induced HMGB1 expression.

10. Alteration in HMGB1 levels following Slug siRNA transfection

To determine the relationship between HMGB1 and Slug, alterations in HMGB1 mRNA level was detected following Slug siRNA transfection. It was found that the HMGB1 level was markedly decreased at 24 h post-transfection. HMGB1 mRNA decreased to 76% at 24 h after transfection (Figure 11). There was a statistically significant difference between scrambled siRNA and Slug siRNA expression levels ($p < 0.05$).

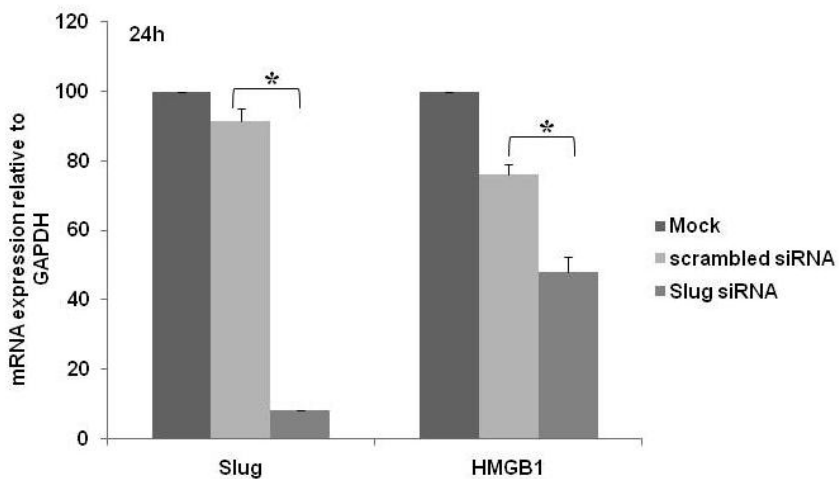


Figure 11. Down-regulation of HMGB1 after Slug siRNA transfection. The HMGB1 level was markedly decreased at 24 h post-transfection of Slug siRNA ($*p < 0.05$).

11. Addition of recombinant HMGB1 accelerates HaCaT cell migration

The ability of recombinant HMGB1 to modify the migration rate of HaCaT cells was tested by using a scratch assay. Cells were treated with either 0.5 μg or 1 μg of recombinant HMGB1. As shown in Figure 12, 0.5 μg and 1 μg of HMGB1 were able to significantly accelerate the rate of cell migration in HaCaT cells.

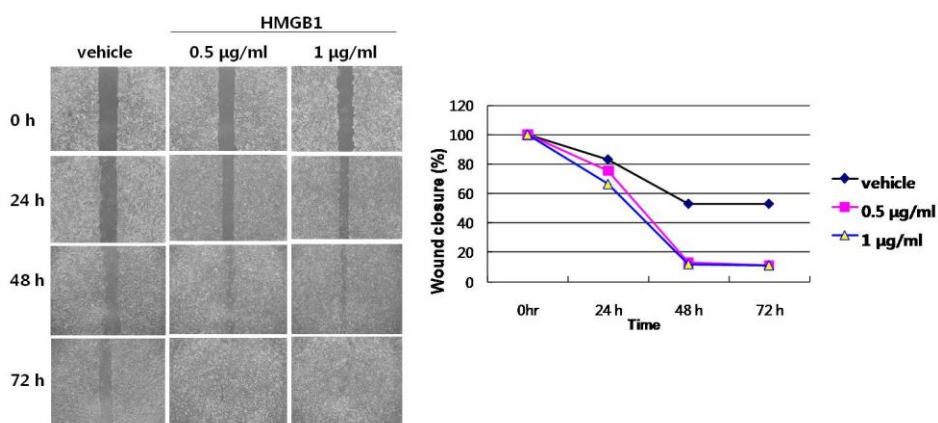


Figure 12. Increased migration of HaCaT cells after treatment with HMGB1. Confluent HaCaT cells were wounded, and re-epithelialization was evaluated in untreated cells and in cells incubated with 0.5 or 1.0 $\mu\text{g/ml}$ HMGB1 at indicated time points. The migration of HaCaT cells was increased after treatment with HMGB1 in a dose-dependent manner.

12. HMGB1 is important in the migration of HaCaT cells

To determine whether HMGB1 is involved in HaCaT cell migration, cells were transfected with HMGB1 siRNA. After 24 h of transfection with 10, 20, or 30 nM siRNA, the mRNA level of HMGB1 was significantly decreased by 25%, 41%, and 70%, respectively ($p < 0.05$), as compared with the scrambled siRNA group (Figure 13a). Using a scratch assay, the migration of HaCaT cells was markedly inhibited by transfection with HMGB1 siRNA as compared to cells transfected with scrambled siRNA (Figure 13b).

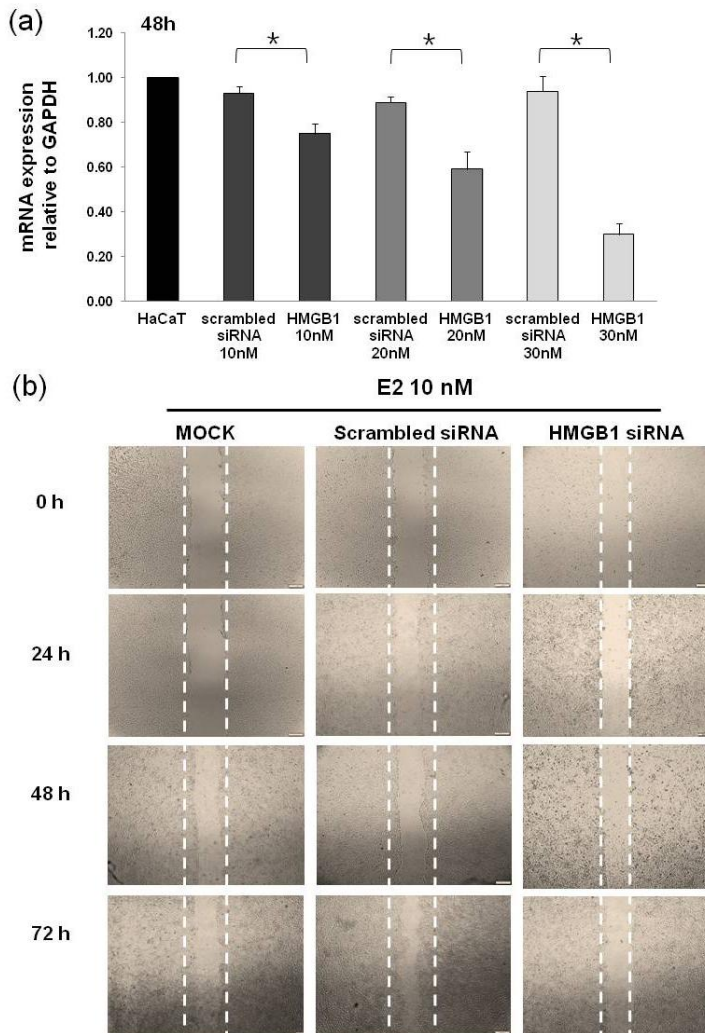


Figure 13. Knockdown of HMGB1 inhibits the migration of HaCaT cells. (a) The expression of HMGB1 was down-regulated by HMGB1 siRNA transfection. HMGB1 mRNA levels were determined by qRT-PCR ($*p < 0.05$). (b) The migration of HaCaT cells was inhibited significantly corresponding to the down-regulation of HMGB1.

IV. DISCUSSION

Epithelial-mesenchymal transition, or EMT, is characterized by molecular changes that lead to an alteration in cell phenotype from stationary to motile^{37,38}. EMT has been implicated not only in embryogenesis and cancer metastasis, but also in the normal wound healing process. In the wound healing process, induction of fibroblasts from epithelia has been proposed as a Type II EMT^{39,40}; EMT associated with cancer metastasis is Type III and that associated with embryogenesis is Type I. Keratinocyte re-epithelialization, another important process in wound healing, and EMT share many similarities at the molecular level, including growth factor responses, signaling pathways, transcriptional/post transcriptional regulation, and cellular/extracellular matrix interactions⁴¹. Both processes also involve phenotypic changes from stationary to motile. This EMT-like change in keratinocytes has been reported to be activated by various stimuli such as UV irradiation²⁸, EGF²⁹, TGF- β ^{28,30-32}, and TNF- α ³².

Estrogen has been reported to accelerate wound healing via accelerated re-epithelialization of keratinocytes^{13,42,43} and to promote cancer metastasis, especially in breast cancer^{44,45}. Recently, the relationship between estrogen and EMT has been studied in other tissues and cancers⁴⁶⁻⁴⁸; however, it has not been studied in keratinocytes. Therefore, it could be speculated that estrogen may activate and mobilize keratinocytes in wound healing in a manner that is

reminiscent of EMT.

In this study, estrogen modulated EMT-related molecules in HaCaT cells. Increased expression of Slug, a strong inducer of EMT, was necessary for HaCaT cell migration. Moreover, using SILAC-based mass spectrometry, HMGB1 was found to be up-regulated after estrogen treatment, and was necessary for HaCaT cell migration. Knockdown experiments using Slug siRNA showed that HMGB1 expression might be related to Slug.

Keratinocyte migration directly contributes to the closure of skin wounds⁴⁹. Savagner et al.⁵⁰ analyzed the expression of Slug during wound healing by using *in situ* hybridization and reported a crucial role for Slug in keratinocyte migration *in vitro*. Hudson et al.⁵¹ also showed that re-epithelialization of excisional wound healing was significantly impaired in Slug-deficient mice. In addition, EGF, the most potent effector of keratinocyte migration, induced activation of ERK5 and up-regulated Slug, the key transcription factor in EMT²⁹. During wound healing, estrogen influences skin wound healing by modulating the inflammatory response^{8,9}, cytokine expression^{10,11}, and extracellular matrix deposition¹², thereby accelerating re-epithelialization¹³ and stimulating angiogenesis¹⁴. Estrogen has a mitogenic effect via the Erk5 pathway on keratinocytes, which increases the rate of re-epithelialization after wounding^{42,43}. Furthermore, estrogen has been reported to stimulate the migration of keratinocytes⁵². However, the downstream mechanism of how estrogen promotes re-epithelialization remains to be elucidated.

The estrogen-induced molecular changes demonstrated in this study are consistent with changes seen during EMT. EMT-related transcription factors, such as Slug and Twist, were up-regulated after estrogen treatment. E-cadherin, an epidermal marker, was down-regulated, while vimentin, a mesenchymal marker, was up-regulated following estrogen treatment. Estrogen accelerated keratinocyte migration and this effect was lost upon Slug knockdown. The Snail family of transcription factors is best known for its ability to trigger EMT through the repression of E-cadherin⁵³⁻⁵⁵. They are also involved in the modulation of tight junction proteins, matrix metalloproteinases, and cytokeratins. High expression of Slug is often found at the wound edge⁵⁰. From the present data, it appears that estrogen might promote re-epithelialization in wound healing via an EMT-like process, which leads to the down-regulation of E-cadherin.⁵⁰

SILAC is a simple and powerful quantitative proteomics method to characterize proteins by mass spectrometry⁵⁶. Using SILAC, thousands of peptides from complex mixtures can be analyzed and quantified. In this study, SILAC was used to find a novel protein associated with estrogen-induced EMT, and 1085 proteins were identified. Among the 60 up-regulated proteins, 6 high mobility group (HMG) proteins were found.

HMG proteins were first discovered 40 years ago⁵⁷. Their roles have been investigated in the nucleus and mitochondria as DNA-binding proteins, and in the cytoplasm as signaling regulators, and most recently, in the extracellular

environment as inflammatory cytokines. The HMG proteins are divided into three families^{58,59}: HMG-A⁶⁰, HMG-N⁶¹, and HMG box (HMGB)⁶²⁻⁶⁶ proteins. HMGB proteins are the largest group and play essential roles as DNA-binding proteins to recognize DNA and mediate DNA-dependent cellular processes^{65,66}. Among the HMGB proteins, HMGB1 has been found to be released into the extracellular space and act as a cytokine to mediate inflammation, in addition to its role in the nucleus⁶⁷⁻⁷². As an extracellular inflammatory mediator, HMGB1 has been implicated to play an important role in wound healing in previous studies⁷³⁻⁷⁶. HMGB1 can induce keratinocyte migration⁷⁴ and act as a chemo-attractant for inflammatory cells⁷⁶. HMGB1 also acts as a mitogen in several cell types and recruits stem cells to promote tissue regeneration^{75,77-79}. In this study, after stimulation with estrogen, not only the expression of HMGB1 in keratinocytes but also the secretion of HMGB1 from keratinocytes was increased. Recombinant HMGB1 treatment increased the migration of HaCaT cells. Knockdown of HMGB1 using HMGB1 siRNA transfection blocked the estrogen-induced migration of HaCaT cells. In addition, HMGB1 was decreased after transfection with Slug siRNA. These results suggest that HMGB1 plays a crucial role in keratinocyte migration, and that this can be related to Slug expression.

Estrogen plays a well-known role in aging. In the skin, the role of estrogen in aging has been analyzed in many studies. Estrogen is strongly related to

chronological aging, as estrogen affects skin thickness and collagen content. Estrogen prevents skin aging by influencing skin wrinkling and moisture, and skin appendages, such as hair^{1-5,80}. Interestingly, EMT and aging are strongly intertwined, although it remains to be established whether the two processes are mechanistically tied together⁸¹. For example, one of the most important transcription factors in EMT, Zeb1, is also related to aging. Depletion of Zeb1 causes mesenchymal-epithelial transition (MET) and triggers premature senescence, whereas Zeb1 is thought to drive cancer progression by promoting EMT and inhibiting senescence^{82,83}. HMGB1 has also been shown to play an important role in maintaining telomere integrity in mammalian cells⁷³. As shown in this study, estrogen, Slug, and HMGB1 were related to each other. Based on these results, the implication that skin aging is associated with EMT and/or HMGB1 should be investigated in further study.

In summary, the study herein showed that estrogen can enhance keratinocyte motility by triggering EMT-like molecular changes, and that this effect might be mediated by HMGB1. Further investigation is necessary to confirm the relationship between HMGB1 and Slug. These relationships among estrogen, EMT, and HMGB1 can be applied to research of other processes, such as aging or cancer metastasis. Furthermore, among the 1085 proteins identified by SILAC analysis, other proteins must be further validated to better understand the role of estrogen in the skin.

V. CONCLUSION

The effects of estrogen on EMT in keratinocytes were evaluated in HaCaT cells. Using SILAC, further investigation to discover novel proteins that link EMT and keratinocyte migration was performed.

1. Estrogen up-regulated the expression of Slug, Twist, and Vimentin in HaCaT cells.
2. Estrogen down-regulated the expression of E-cadherin in HaCaT cells.
3. The changes in these molecules were reversed following treatment with ICI, an estrogen receptor antagonist.
4. Increased migration of HaCaT cells following estrogen treatment was reversed by Slug siRNA transfection.
5. Using SILAC, 1085 proteins were identified in HaCaT cells.
6. Among the 1085 proteins, 32 proteins were down-regulated and 60 proteins were up-regulated with estrogen treatment.
7. HMGB1 expression was increased after estrogen treatment, and increased HMGB1 was reversed after treatment with ICI.
8. HMGB1 was down-regulated after Slug siRNA transfection.
9. The migration of HaCaT cells was increased after treatment with the recombinant HMGB1 protein.
10. The migration of HaCaT cells was reversed by HMGB1 siRNA

transfection.

11. Knockdown of Slug in keratinocytes resulted in a significant decrease in HMGB1.

Based on these results, it is anticipated that estrogen is a potent inducer of EMT in keratinocytes. Furthermore, HMGB1 may be a novel protein that mediates the effect of estrogen on keratinocytes. Further investigation is necessary to confirm the relationship between HMGB1 and Slug. In addition, among the 1085 proteins identified by the SILAC analysis, other proteins must be further validated to understand the role of estrogen in the skin.

REFERENCES

1. Hall GK, Phillips TJ. Skin and hormone therapy. *Clin Obstet Gynecol* 2004;47:437-49.
2. Kanda N, Watanabe S. Regulatory roles of sex hormones in cutaneous biology and immunology. *J Dermatol Sci* 2005;38:1-7.
3. Phillips TJ, Demircay Z, Sahu M. Hormonal effects on skin aging. *Clin Geriatr Med* 2001;17:661-72, vi.
4. Raine-Fenning NJ, Brincat MP, Muscat-Baron Y. Skin aging and menopause : implications for treatment. *Am J Clin Dermatol* 2003;4:371-8.
5. Sator PG, Schmidt JB, Sator MO, Huber JC, Honigsmann H. The influence of hormone replacement therapy on skin ageing: a pilot study. *Maturitas* 2001;39:43-55.
6. Ashcroft GS, Ashworth JJ. Potential role of estrogens in wound healing. *Am J Clin Dermatol* 2003;4:737-43.
7. Calvin M. Oestrogens and wound healing. *Maturitas* 2000;34:195-210.
8. Ashcroft GS, Greenwell-Wild T, Horan MA, Wahl SM, Ferguson MW. Topical estrogen accelerates cutaneous wound healing in aged humans associated with an altered inflammatory response. *Am J Pathol* 1999;155:1137-46.
9. Mills SJ, Ashworth JJ, Gilliver SC, Hardman MJ, Ashcroft GS. The

- sex steroid precursor DHEA accelerates cutaneous wound healing via the estrogen receptors. *J Invest Dermatol* 2005;125:1053-62.
10. Ashcroft GS, Mills SJ, Lei K, Gibbons L, Jeong MJ, Taniguchi M, et al. Estrogen modulates cutaneous wound healing by downregulating macrophage migration inhibitory factor. *J Clin Invest* 2003;111:1309-18.
 11. Ashcroft GS, Mills SJ, Flanders KC, Lyakh LA, Anzano MA, Gilliver SC, et al. Role of Smad3 in the hormonal modulation of in vivo wound healing responses. *Wound Repair Regen* 2003;11:468-73.
 12. Ashcroft GS, Yang X, Glick AB, Weinstein M, Letterio JL, Mizel DE, et al. Mice lacking Smad3 show accelerated wound healing and an impaired local inflammatory response. *Nat Cell Biol* 1999;1:260-6.
 13. Ashcroft GS, Dodsworth J, van Boxtel E, Tarnuzzer RW, Horan MA, Schultz GS, et al. Estrogen accelerates cutaneous wound healing associated with an increase in TGF-beta1 levels. *Nat Med* 1997;3:1209-15.
 14. Morales DE, McGowan KA, Grant DS, Maheshwari S, Bhartiya D, Cid MC, et al. Estrogen promotes angiogenic activity in human umbilical vein endothelial cells in vitro and in a murine model. *Circulation* 1995;91:755-63.
 15. Kong W, Li S, Liu C, Bari AS, Longaker MT, Lorenz HP. Epithelial-mesenchymal transition occurs after epidermal development in mouse

- skin. *Exp Cell Res* 2006;312:3959-68.
16. Jamora C, Lee P, Kocieniewski P, Azhar M, Hosokawa R, Chai Y, et al. A signaling pathway involving TGF-beta2 and snail in hair follicle morphogenesis. *PLoS Biol* 2005;3:e11.
 17. Magnoni C, Giudice S, Pellacani G, Bertazzoni G, Longo C, Veratti E, et al. Stem Cell Properties in Cell Cultures From Different Stage of Melanoma Progression. *Appl Immunohistochem Mol Morphol* 2013.
 18. Qu X, Shen L, Zheng Y, Cui Y, Feng Z, Liu F, et al. A Signal Transduction Pathway from TGF-beta1 to SKP2 via Akt1 and c-Myc and Its Correlation with Progression in Human Melanoma. *J Invest Dermatol* 2013.
 19. Shimokawa M, Haraguchi M, Kobayashi W, Higashi Y, Matsushita S, Kawai K, et al. The transcription factor Snail expressed in cutaneous squamous cell carcinoma induces epithelial-mesenchymal transition and down-regulates COX-2. *Biochem Biophys Res Commun* 2013;430:1078-82.
 20. Wong CE, Yu JS, Quigley DA, To MD, Jen KY, Huang PY, et al. Inflammation and Hras signaling control epithelial-mesenchymal transition during skin tumor progression. *Genes Dev* 2013;27:670-82.
 21. Arnoux V, Nassour M, L'Helgoualc'h A, Hipskind RA, Savagner P. Erk5 controls Slug expression and keratinocyte activation during wound healing. *Mol Biol Cell* 2008;19:4738-49.

22. Hudson LG, Newkirk KM, Chandler HL, Choi C, Fossey SL, Parent AE, et al. Cutaneous wound reepithelialization is compromised in mice lacking functional Slug (Snai2). *J Dermatol Sci* 2009;56:19-26.
23. Kusewitt DF, Choi C, Newkirk KM, Leroy P, Li Y, Chavez MG, et al. Slug/Snai2 is a downstream mediator of epidermal growth factor receptor-stimulated reepithelialization. *J Invest Dermatol* 2009;129:491-5.
24. Savagner P, Kusewitt DF, Carver EA, Magnino F, Choi C, Gridley T, et al. Developmental transcription factor slug is required for effective re-epithelialization by adult keratinocytes. *J Cell Physiol* 2005;202:858-66.
25. Takahashi M, Akamatsu H, Yagami A, Hasegawa S, Ohgo S, Abe M, et al. Epithelial-mesenchymal transition of the eccrine glands is involved in skin fibrosis in morphea. *J Dermatol* 2013.
26. Iwano M, Plieth D, Danoff TM, Xue C, Okada H, Neilson EG. Evidence that fibroblasts derive from epithelium during tissue fibrosis. *J Clin Invest* 2002;110:341-50.
27. Postlethwaite AE, Shigemitsu H, Kanangat S. Cellular origins of fibroblasts: possible implications for organ fibrosis in systemic sclerosis. *Curr Opin Rheumatol* 2004;16:733-8.
28. Li Y, Liu Y, Xu Y, Voorhees JJ, Fisher GJ. UV irradiation induces Snail expression by AP-1 dependent mechanism in human skin

- keratinocytes. *J Dermatol Sci* 2010;60:105-13.
29. Arnoux V, Nassour M, L'Helgoualc'h A, Hippskind RA, Savagner P. Erk5 controls Slug expression and keratinocyte activation during wound healing. *Mol Biol Cell* 2008;19:4738-49.
 30. Davies M, Robinson M, Smith E, Huntley S, Prime S, Paterson I. Induction of an epithelial to mesenchymal transition in human immortal and malignant keratinocytes by TGF-beta1 involves MAPK, Smad and AP-1 signalling pathways. *J Cell Biochem* 2005;95:918-31.
 31. Santibanez JF. JNK mediates TGF-beta1-induced epithelial mesenchymal transdifferentiation of mouse transformed keratinocytes. *FEBS Lett* 2006;580:5385-91.
 32. Yan C, Grimm WA, Garner WL, Qin L, Travis T, Tan N, et al. Epithelial to mesenchymal transition in human skin wound healing is induced by tumor necrosis factor-alpha through bone morphogenic protein-2. *Am J Pathol* 2010;176:2247-58.
 33. Washburn MP, Wolters D, Yates JR, 3rd. Large-scale analysis of the yeast proteome by multidimensional protein identification technology. *Nat Biotechnol* 2001;19:242-7.
 34. Carvalho PC, Xu T, Han X, Cociorva D, Barbosa VC, Yates JR, 3rd. YADA: a tool for taking the most out of high-resolution spectra. *Bioinformatics* 2009;25:2734-6.
 35. Tabb DL, McDonald WH, Yates JR, 3rd. DTASelect and Contrast:

- tools for assembling and comparing protein identifications from shotgun proteomics. *J Proteome Res* 2002;1:21-6.
36. Thornton MJ. The biological actions of estrogens on skin. *Exp Dermatol* 2002;11:487-502.
 37. Savagner P. The epithelial-mesenchymal transition (EMT) phenomenon. *Ann Oncol* 2010;21 Suppl 7:vii89-92.
 38. Chaffer CL, Weinberg RA. A perspective on cancer cell metastasis. *Science* 2011;331:1559-64.
 39. Kalluri R, Weinberg RA. The basics of epithelial-mesenchymal transition. *J Clin Invest* 2009;119:1420-8.
 40. Zeisberg M, Neilson EG. Biomarkers for epithelial-mesenchymal transitions. *J Clin Invest* 2009;119:1429-37.
 41. Leopold PL, Vincent J, Wang H. A comparison of epithelial-to-mesenchymal transition and re-epithelialization. *Semin Cancer Biol* 2012;22:471-83.
 42. Kanda N, Watanabe S. 17beta-estradiol stimulates the growth of human keratinocytes by inducing cyclin D2 expression. *J Invest Dermatol* 2004;123:319-28.
 43. Verdier-Sevrain S, Yaar M, Cantatore J, Traish A, Gilchrist BA. Estradiol induces proliferation of keratinocytes via a receptor mediated mechanism. *FASEB J* 2004;18:1252-4.
 44. Platet N, Cathiard AM, Gleizes M, Garcia M. Estrogens and their

- receptors in breast cancer progression: a dual role in cancer proliferation and invasion. *Crit Rev Oncol Hematol* 2004;51:55-67.
45. Rochefort H, Platet N, Hayashido Y, Derocq D, Lucas A, Cunat S, et al. Estrogen receptor mediated inhibition of cancer cell invasion and motility: an overview. *J Steroid Biochem Mol Biol* 1998;65:163-8.
 46. Guttilla IK, Adams BD, White BA. ERalpha, microRNAs, and the epithelial-mesenchymal transition in breast cancer. *Trends Endocrinol Metab* 2012;23:73-82.
 47. Scherbakov AM, Andreeva OE, Shatskaya VA, Krasil'nikov MA. The relationships between snail1 and estrogen receptor signaling in breast cancer cells. *J Cell Biochem* 2012;113:2147-55.
 48. Wang KH, Kao AP, Lin TC, Chang CC, Kuo TC. Promotion of epithelial-mesenchymal transition and tumor growth by 17beta-estradiol in an ER(+)/HER2(+) cell line derived from human breast epithelial stem cells. *Biotechnol Appl Biochem* 2012;59:262-7.
 49. Coulombe PA. Wound epithelialization: accelerating the pace of discovery. *J Invest Dermatol* 2003;121:219-30.
 50. Savagner P, Kusewitt DF, Carver EA, Magnino F, Choi C, Gridley T, et al. Developmental transcription factor slug is required for effective re-epithelialization by adult keratinocytes. *J Cell Physiol* 2005;202:858-66.
 51. Hudson LG, Newkirk KM, Chandler HL, Choi C, Fossey SL, Parent

- AE, et al. Cutaneous wound reepithelialization is compromised in mice lacking functional Slug (Snai2). *J Dermatol Sci* 2009;56:19-26.
52. Merlo S, Frasca G, Canonico PL, Sortino MA. Differential involvement of estrogen receptor alpha and estrogen receptor beta in the healing promoting effect of estrogen in human keratinocytes. *J Endocrinol* 2009;200:189-97.
53. Batlle E, Sancho E, Franci C, Dominguez D, Monfar M, Baulida J, et al. The transcription factor snail is a repressor of E-cadherin gene expression in epithelial tumour cells. *Nat Cell Biol* 2000;2:84-9.
54. Bolos V, Peinado H, Perez-Moreno MA, Fraga MF, Esteller M, Cano A. The transcription factor Slug represses E-cadherin expression and induces epithelial to mesenchymal transitions: a comparison with Snail and E47 repressors. *J Cell Sci* 2003;116:499-511.
55. Cano A, Perez-Moreno MA, Rodrigo I, Locascio A, Blanco MJ, del Barrio MG, et al. The transcription factor snail controls epithelial-mesenchymal transitions by repressing E-cadherin expression. *Nat Cell Biol* 2000;2:76-83.
56. Mann M. Functional and quantitative proteomics using SILAC. *Nat Rev Mol Cell Biol* 2006;7:952-8.
57. Goodwin GH, Sanders C, Johns EW. A new group of chromatin-associated proteins with a high content of acidic and basic amino acids. *Eur J Biochem* 1973;38:14-9.

58. Bustin M. Revised nomenclature for high mobility group (HMG) chromosomal proteins. *Trends Biochem Sci* 2001;26:152-3.
59. Reeves R. Nuclear functions of the HMG proteins. *Biochim Biophys Acta* 2010;1799:3-14.
60. Sgarra R, Zammitti S, Lo Sardo A, Maurizio E, Arnoldo L, Pegoraro S, et al. HMGA molecular network: From transcriptional regulation to chromatin remodeling. *Biochim Biophys Acta* 2010;1799:37-47.
61. Gerlitz G. HMGNs, DNA repair and cancer. *Biochim Biophys Acta* 2010;1799:80-5.
62. Asin-Cayuela J, Gustafsson CM. Mitochondrial transcription and its regulation in mammalian cells. *Trends Biochem Sci* 2007;32:111-7.
63. Bianchi ME, Agresti A. HMG proteins: dynamic players in gene regulation and differentiation. *Curr Opin Genet Dev* 2005;15:496-506.
64. Bonawitz ND, Clayton DA, Shadel GS. Initiation and beyond: multiple functions of the human mitochondrial transcription machinery. *Mol Cell* 2006;24:813-25.
65. Stros M. HMGB proteins: interactions with DNA and chromatin. *Biochim Biophys Acta* 2010;1799:101-13.
66. Thomas JO. HMG1 and 2: architectural DNA-binding proteins. *Biochem Soc Trans* 2001;29:395-401.
67. Agresti A, Bianchi ME. HMGB proteins and gene expression. *Curr Opin Genet Dev* 2003;13:170-8.

68. Bianchi ME, Beltrame M, Paonessa G. Specific recognition of cruciform DNA by nuclear protein HMG1. *Science* 1989;243:1056-9.
69. Giese K, Cox J, Grosschedl R. The HMG domain of lymphoid enhancer factor 1 bends DNA and facilitates assembly of functional nucleoprotein structures. *Cell* 1992;69:185-95.
70. Andersson U, Wang H, Palmblad K, Aveberger AC, Bloom O, Erlandsson-Harris H, et al. High mobility group 1 protein (HMG-1) stimulates proinflammatory cytokine synthesis in human monocytes. *J Exp Med* 2000;192:565-70.
71. Scaffidi P, Misteli T, Bianchi ME. Release of chromatin protein HMGB1 by necrotic cells triggers inflammation. *Nature* 2002;418:191-5.
72. Wang H, Bloom O, Zhang M, Vishnubhakat JM, Ombrellino M, Che J, et al. HMG-1 as a late mediator of endotoxin lethality in mice. *Science* 1999;285:248-51.
73. Polanska E, Dobsakova Z, Dvorackova M, Fajkus J, Stros M. HMGB1 gene knockout in mouse embryonic fibroblasts results in reduced telomerase activity and telomere dysfunction. *Chromosoma* 2012;121:419-31.
74. Ranzato E, Patrone M, Pedrazzi M, Burlando B. HMGB1 promotes scratch wound closure of HaCaT keratinocytes via ERK1/2 activation. *Mol Cell Biochem* 2009;332:199-205.

75. Straino S, Di Carlo A, Mangoni A, De Mori R, Guerra L, Maurelli R, et al. High-mobility group box 1 protein in human and murine skin: involvement in wound healing. *J Invest Dermatol* 2008;128:1545-53.
76. Zhang Q, O'Hearn S, Kavalukas SL, Barbul A. Role of high mobility group box 1 (HMGB1) in wound healing. *J Surg Res* 2012;176:343-7.
77. Chavakis E, Hain A, Vinci M, Carmona G, Bianchi ME, Vajkoczy P, et al. High-mobility group box 1 activates integrin-dependent homing of endothelial progenitor cells. *Circ Res* 2007;100:204-12.
78. Naglova H, Bucova M. HMGB1 and its physiological and pathological roles. *Bratisl Lek Listy* 2012;113:163-71.
79. Palumbo R, Sampaolesi M, De Marchis F, Tonlorenzi R, Colombetti S, Mondino A, et al. Extracellular HMGB1, a signal of tissue damage, induces mesoangioblast migration and proliferation. *J Cell Biol* 2004;164:441-9.
80. Thornton MJ. Oestrogen functions in skin and skin appendages. *Expert Opin Ther Targets* 2005;9:617-29.
81. Smit MA, Peeper DS. Epithelial-mesenchymal transition and senescence: two cancer-related processes are crossing paths. *Aging (Albany NY)* 2010;2:735-41.
82. Brabletz S, Brabletz T. The ZEB/miR-200 feedback loop--a motor of cellular plasticity in development and cancer? *EMBO Rep* 2010;11:670-7.

83. Liu Y, El-Naggar S, Darling DS, Higashi Y, Dean DC. Zeb1 links epithelial-mesenchymal transition and cellular senescence. *Development* 2008;135:579-88.

ABSTRACT (IN KOREAN)

각질형성세포에서 에스트로겐에 의한 상피세포-중간엽세포
이행과 창상치유에 관한 연구

<지도교수 이광훈>

연세대학교 대학원 의학과

신 정 우

피부에 노화가 오면 상처 치유가 지연되게 된다. 특히 여성에서는 에스트로겐의 분비가 저하되는 폐경 이후에 이런 변화가 뚜렷하게 되는데 폐경 여성에서 에스트로겐을 보충해 주면 상처 치유가 촉진되며 이 과정에 각질형성세포의 이주 증가가 중요한 역할을 한다. 또한 상피세포-중간엽세포 이행은 각질형성세포의 이주 증가와도 연관되어 있음이 알려져 있다. 그러나 에스트로겐이 상피세포-중간엽세포 이행을 통해 각질형성세포의 이주 증가를 촉진하는지 또 이 과정에 어떤 분자가 관여하는지는 아직 명확히 밝혀져 있지 않다.

이에 이 연구에서는 첫째, 에스트로겐에 의한 각질형성세포의 이주 증가가 상피세포-중간엽세포 이행과 관련되어 있는지 관찰하였고, 둘째, 이 과정에 관여하는 신 물질을 발굴하고자 stable isotope labeling by amino acids in cell culture (SILAC)을 시행하였다.

연구자는 배양한 HaCaT 세포와 사람각질형성세포에서 에스트로겐 수용체 β 만 발현됨을 관찰하였다. 배양한 HaCaT 세포에 0.1, 1, 10, 100 nM 의 에스트로겐을 48 시간 처치 후 시행한 qRT-PCR, western

blot, 직접면역형광검사에서 Slug 와 Twist 가 농도 의존성으로 유의하게 증가하였고 vimentin 또한 증가하였으나 E-cadherin 은 감소하였다. 에스트로겐 수용체 길항제인 ICI 처치 후 시행한 qRT-PCR 에서 에스트로겐에 의한 Slug, Twist, vimentin 의 발현 증가가 유의하게 억제되었다. 에스트로겐을 처치 후 시행한 wound scratch assay 와 transwell assay 에서 HaCaT 세포의 이주가 통계적으로 유의하게 증가하였다. siRNA 를 이용하여 Slug 를 knockdown 시킨 HaCaT 세포에서는 에스트로겐에 의한 세포의 이주 증가가 억제되었고 vimentin 과 E-cadherin 의 발현 변화가 유의하게 억제되었다.

배양한 HaCaT 세포의 SILAC 분석 결과 1,085 개의 단백질이 관찰되었고 100 nM 에스트로겐을 48 시간 처치한 HaCaT 세포에서 처치하지 않은 세포에 비해 32 개의 단백질이 유의하게 감소되었으며 60 개의 단백질이 유의하게 증가되었다. 60 개의 증가된 단백질 중 6 개의 high-mobility group protein 이 유의하게 증가되었다.

배양한 HaCaT 세포에서 에스트로겐 처치 후 시행한 qRT-PCR 과 western blot 에서 HMGB1 의 발현이 유의하게 증가하였으며 이러한 변화는 ICI 처치 후 억제되었다. Slug 를 knockdown 시킨 HaCaT 세포에서 HMGB1 의 발현이 qRT-PCR 결과 통계적으로 유의하게 감소하였다. HaCaT 세포에 HMGB1 처치 후 세포의 이주가 증가하였으며 HMGB1 을 knockdown 시킨 HaCaT 세포에서는 에스트로겐에 의한 세포의 이주 증가가 억제되었다.

이상의 결과를 통하여 에스트로겐이 각질형성세포의 이주를 증가시키며 이는 상피세포-중간엽세포 이행과 관련되어 있음을 관찰할 수 있었다. 또한 에스트로겐 처치 후 HMGB1 의 발현

증가가 에스트로겐에 의한 HaCaT 세포의 이주 증가에 중요한 역할을 하고 상피세포-중간엽세포 이행과도 연관 되어 있을 것으로 생각된다.

핵심되는 말: 에스트로겐, 각질형성세포, 이주, 상피세포-중간엽세포 이행, HMGB1, SILAC